EXPERIMENTAL EVALUATION OF A LINEAR-POLAR-DISPLAY SIGNAL ANALYZER

Norbert James Spitzer

United States Naval Postgraduate School

THESIS

EXPERIMENTAL EVALUATION
OF A
LINEAR POLAR-DISPLAY SIGNAL ANALYZER

by

Norbert James Spitzer

June 1969

Experimental Evaluation
of a
Linear Polar-Display Signal Analyzer

by

Norbert James Spitzer
Major, United States Marine Corps
B. S. Physics, University of Notre Dame, 1960

Submitted in partial fulfillment of the
requirements for the degree of

ELECTRICAL ENGINEER

from the

NAVAL POSTGRADUATE SCHOOL
June 1969

ABSTRACT

This report presents the results of an experimental evaluation of a linear, polar-display signal analyzer. Signals generated in the laboratory are used to determine the ability of the device to indicate the type of carrier modulation and the carrier parameters such as frequency, data rate, and bandwidth. Live signals in the HF band are monitored by applying the predetected output of an R-390A receiver directly to the signal analyzer.

Photographs of the actual displays resulting from signals generated in the laboratory demonstrate the ability of the system to provide a distinctive display in each case. Various parameters of the input signal can be determined by measuring parameters of the display. A twelve minute movie indicates the system performance in the case of live signals. The ability of the signal analyzer to determine the normalized autocorrelation function of a bandpass gaussian process is demonstrated.

Data contained in this thesis has been published as Technical Report NPS-52MV9071A. AD No. 696 569.

TABLE OF CONTENTS

LIST OF ILLUSTRATIONS

LIST OF SYMBOLS

a	Dimension of the semi-major axis of an ellipse
b	Dimension of the semi-minor axis of an ellipse
$d(t)$	Modulating data for digital modulation
e_i	Input signal
e_o	Output signal
f	Frequency in Hertz
f_c	Carrier frequency in Hertz
f_i	Instantaneous carrier frequency in Hertz
f_m	Hertzian frequency of the modulating signal
f_o	Center frequency in Hertz
g_{fs}	Transconductance of a field-effect transistor
h_{fe}	Forward current transfer ratio for a transistor in the common-emitter configuration
k_f	Frequency modulator constant
k_p	Phase modulator constant
m	Modulation index of amplitude modulation
$n(t)$	Narrowband gaussian process
r_{ce}	Resistance seen between the collector and the emitter of a transistor
$v(t)$	Carrier signal
A	A constant = amplitude of the modulating function
$E(t)$	Envelope of the carrier
$E_m(t)$	Modulating signal for single-sideband transmissions
K	A constant = amplitude of the unmodulated carrier

$S(t)$	Switching function
T_p	Period of a periodic function
$\alpha(t)$	Carrier angle modulation
θ	Angular coordinate of the oscilloscope trace
θ_d	Angle of rotation of the coordinate axes
ρ	Radial coordinate of the oscilloscope trace
$\overline{\rho}$	Normalized autocorrelation function
$\sigma(t)$	Hilbert transform of $E_m(t)$
τ	System delay
ϕ	Carrier phase
ω	Radian frequency = $2\pi f$
ω_c	$2\pi f_c$
ω_i	$2\pi f_i$
ω_m	$2\pi f_m$
ω_o	$2\pi f_o$

ACKNOWLEDGEMENT

The author wishes to express his appreciation for the efforts of Professor G. A. Myers without whose guidance, encouragement and assistance this report would never have come about.

I. INTRODUCTION

Various parameters can be used to characterize radio signals. Some of these are:

(1) average carrier frequency
(2) carrier envelope
(3) carrier instantaneous phase
(4) carrier instantaneous frequency
(5) type of modulation
(6) bandwidth or Fourier spectrum
(7) duty factor (pulsed signals).

A measure of each of these descriptors is normally obtained in a sequential manner. An apparatus which provides simultaneously an indication of several of these parameters and which presents this information in the form of a visual display has obvious applications. Such a device could be used as a spectrum monitor to obtain information about unknown signals or as a monitor of a known signal to insure adherence to a predetermined format.

Such an apparatus is the Linear Polar-Display (LPD) System considered in this report. Analytical investigations of these systems have been previously reported [Refs. 1 and 2]. The purpose of this study was to build a particular LPD system and to:

(1) verify the display patterns predicted by analysis,
(2) determine and verify the displays produced by pulse-modulated carriers,
(3) investigate the system transient response to various signals,
(4) use the system in conjunction with a standard receiver to determine the system capabilities and limitations in the analysis of live radio signals.

Section II of this report describes the system and explains its operation. The system response is explained in terms of a generalized signal which may possess amplitude modulation or angle modulation or both. The system response to a pure sinusoid is presented as an example of the manner in which the display characterizes a given signal.

Section III presents an analytical description of the system display for each of several common types of signal, such as a full-carrier amplitude-modulated signal, a frequency-modulated signal, a double-sideband, suppressed-carrier signal, and a single-sideband signal. Photographs of actual displays generated by these laboratory signals are included. A study of the ability of the system to measure the normalized autocorrelation function of a gaussian random process is included. This section also describes the procedure followed and presents the results obtained while using the system in conjunction with a receiver to monitor live signals. A movie of the oscilloscope display formed by live signals is available but is not a part of this report.

Conclusions and recommendations are presented in Section IV. A list of references is provided.

Appendix A. contains schematic diagrams of the amplifier and impedance-matching circuits which are a part of the LPD system and of the modulator circuits used to generate the laboratory signals.

II. SYSTEM DESCRIPTION

This section presents a description of the linear signal analyzer and the general nature of its response to an input signal. The dependence of certain display characteristics on signal variables such as carrier level, carrier frequency, and modulation is indicated. The system response to a pure sinusoid is described.

A. PHYSICAL REALIZATION

The system of interest is a dual-channel signal analyzer that can be represented as in Fig. 1.

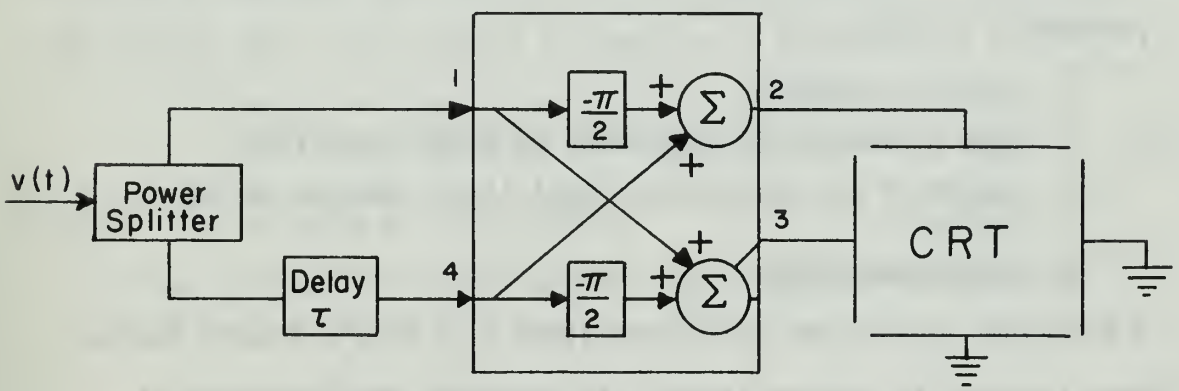

FIG. 1. BLOCK DIAGRAM OF THE LPD SYSTEM.

The signal v(t) is split into two channels. The signal in one channel is delayed relative to that in the other. The delay of τ seconds introduces a frequency-dependent phase shift $\phi = 2\pi f_i \tau$ where f_i is the instantaneous frequency of v(t). Both channels are then passed through a quadrature hybrid junction (QHJ) which is used as a sum-and-difference type of phase-to-amplitude transducer [Ref. 1.].

The QHJ passes the input signal at port 1 directly to port 3. Between ports 1 and 2 a $-\frac{\pi}{2}$ phase shift occurs. The input signal at port 4 is processed in a similar manner as shown in Fig. 1.

The signals at the output ports of the QHJ are applied to the x and y deflection plates of the cathode ray tube to produce the system display. Values of the signal parameters are related to magnitudes of the polar coordinates ρ and θ of the display.

The entire system is linear. No detection, limiting, or other nonlinear action is involved. The signal is processed and displayed in its radio frequency (RF) or intermediate frequency (IF) form.

The resultant display provides information about various signal parameters such as:

1. carrier frequency
2. type of modulation (amplitude or angle modulation)
3. nature of the modulating signal (i.e., whether analog or digital)
4. signal bandwidth.

A system which provides this information in a single display can be used to identify unknown signals, to determine the parameters of unknown signals, or to monitor the parameters of locally generated signals (transmitter output for example).

B. SYSTEM RESPONSE

Consider a generalized signal v(t), having both amplitude and angle modulation. Such a signal can be expressed as

$$v(t) = E(t) \cos[\omega_c t + \alpha(t)] \qquad (1)$$

where E(t) is the carrier envelope, (amplitude modulation), ω_c is the carrier radian frequency, and $\alpha(t)$ is the phase modulation of the carrier.

The system display formed by each cycle of the RF carrier is elliptical in nature [Ref. 1, p. 33]. The size, orientation, and relative magnitudes of the major and minor axes of this "instantaneous ellipse" are functions of the signal strength and the signal modulation. The instantaneous ellipse may degenerate to a line or a circle. Due to the retentivity of the oscilloscope phosphors, the observed trace is composed of many RF cycles. This composite trace, which is called the system display, provides a unique signature for various types of signal of the form given in Eq. (1).

The instantaneous ellipse can be expressed in standard form in terms of coordinate axes x and y which are at an angle θ relative to the display axes. The angle θ of rotation is given by

$$\theta = \frac{\omega_c \tau}{2} + \frac{\pi}{4} + \frac{\alpha(t) - \alpha(t-\tau)}{2} \tag{2}$$

where τ is the value of system delay.[1]

In the rotated coordinate system, the ellipse is expressed as

$$\frac{x^2}{a^2} + \frac{y^2}{b^2} = 1 \tag{3}$$

where

$$a = E(t) + E(t-\tau) \tag{4}$$

and

$$b = E(t) - E(t-\tau) \tag{5}$$

As shown in Fig. 2 the constants a and b are the dimensions of the semi-major and semi-minor axes of the elliptical trace.

---

[1]The displays produced by amplitude-modulated signals contain non-degenerate ellipses. That is, during each RF cycle the polar angle (normally referred to as θ) of the scope trace rotates 2π radians. This report however, defines θ as the angle of rotation of the axes of the instantaneous ellipse.

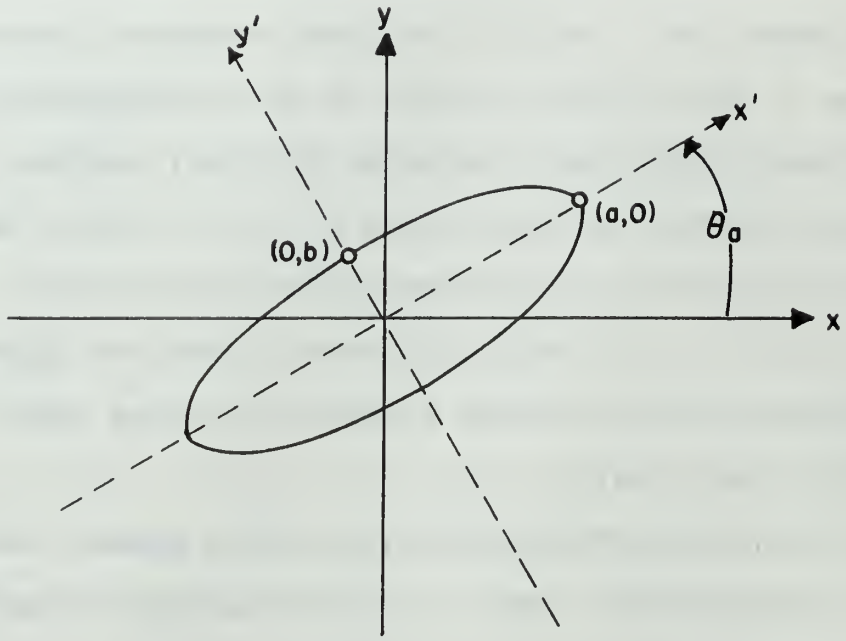

FIG. 2. TYPICAL ELLIPTICAL TRACE GENERATED BY EACH RF CYCLE OF THE SIGNAL APPLIED TO THE LPD SYSTEM.

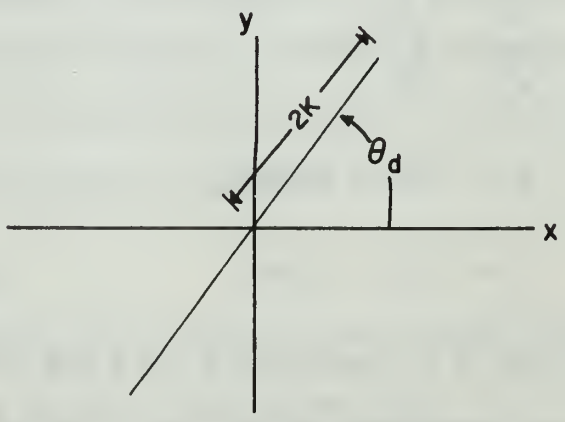

FIG. 3. DIAGRAM OF THE LPD SYSTEM RESPONSE TO AN UNMODULATED SINUSOID.

The system response to a pure sinusoid provides a simple example of the manner in which the display is formed by and hence characterizes a given signal. For this case,

$$v(t) = K \cos \omega_c t. \tag{6}$$

A comparison of Eq. (6) with Eq. (1) indicates that $E(t) = K$, a constant, and $\alpha(t) = 0$. Equation (2) reduces to

$$\theta = \frac{\omega_c \tau}{2} + \frac{\pi}{4} = \theta_d, \text{ a constant.} \tag{7}$$

Since $a = 2K$ from Eq. (4) and $b = 0$ from Eq. (5), the display ellipse degenerates to a straight line of length 4K.

The form of the resultant display is shown in Fig. 3. The signal parameters of interest are related to the polar coordinates ρ and θ of this display as previously suggested. The maximum value of ρ is seen to be equal to a, the length of the semi-major axis. That is, $\rho = a = 2K$. Therefore the maximum value of ρ in this case provides an indication of the strength or level of the input signal. The angle θ_d is a function of carrier frequency and system delay; hence carrier frequency can be determined directly by measurement of θ_d and solution of Eq. (7)

The sensitivity of the system to a change in frequency is given by $\frac{d\theta_d}{d\omega}$. From Eq. (7)

$$\frac{d\theta_d}{d\omega} = \frac{\tau}{2} \quad \text{or} \quad \frac{d\theta_d}{df} = \pi\tau, \text{ a constant.} \tag{8}$$

Therefore, frequency sensitivity is directly proportional to the system delay and is constant with frequency. From Eq. (8) it can be seen that a change in frequency equal to $\frac{1}{\tau}$ is sufficient to cause the display to rotate π radians. Thus the maximum unambiguous bandwidth of the system

is $\frac{1}{\tau}$ Hz. In practice, the unambiguous bandwidth can be increased by reducing τ which also decreases frequency sensitivity.

III. RESULTS

This section presents an analytical description of each of the system displays produced by various signals. The signals are distinguished by the type of modulation (amplitude modulation or angle modulation) and by the nature of the modulating signal (analog or digital). To verify the analytical results, photographs of various oscilloscope displays are included.

An investigation of live signals in the HF band was conducted by obtaining the system input directly from the output of the IF amplifier of an R-390A receiver. As a part of this investigation, a 12 minute, 8mm movie was produced. The movie presents the displays formed by live signals in the HF band as well as those formed by signals generated in the laboratory. The contents of this film are described in detail at the end of this section.

Distinctive displays are formed by various modulated-carrier signals. Figure 4 indicates the displays produced by an amplitude-modulated (AM) carrier, a frequency-modulated (FM) carrier, and a double-sideband suppressed-carrier (AM) signal. In each case the modulating signal is a sinusoid. Figure 5 shows the displays produced by a continuous-wave (CW) carrier, (on-off AM), a frequency-shift-keyed (FSK) carrier, and a phase-shift-keyed (PSK) carrier. In each case, the modulating signal is a square wave.

The photographs of Figs. 4 and 5 indicate the ease with which signals can be classified as to modulation type, and, further, the ease with which a determination can be made as to whether the modulating

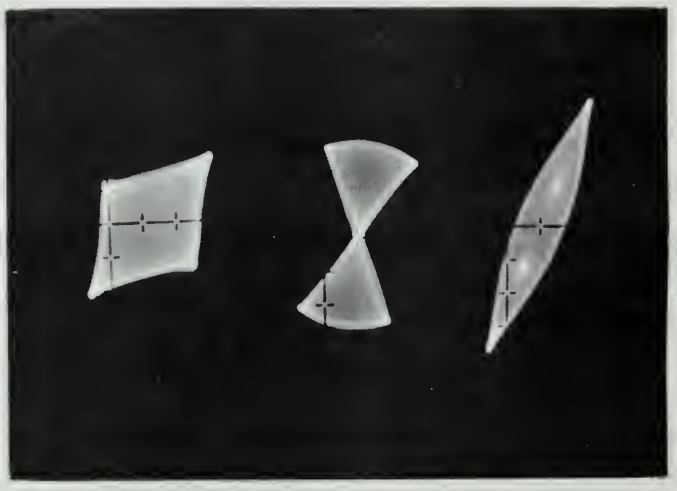

FIG. 4. EXAMPLE OF THE DISPLAYS PRODUCED BY A CARRIER MODULATED BY A 2 kHz SINUSOID. From left to right, the modulation is double-sideband suppressed-carrier AM, FM, and full-carrier AM.

FIG. 5. EXAMPLE OF THE DISPLAYS PRODUCED BY A CARRIER MODULATED BY A SQUARE WAVE. From left to right, the modulation is PSK, FSK, and CW (on-off AM).

signal is digital or analog. Similar distinctive traces are generated for each type of modulation when the modulating signal is an arbitrary time function such as a voice signal (analog case), or a bit stream of data (digital case).

A. ANALYTICAL DESCRIPTION OF THE SYSTEM DISPLAY

In this section the equations which relate parameters of the polar display to the parameters of the applied signal are presented. The equations which describe the display in terms of a generalized signal are given by Eq. (1) - (5).

1. Simultaneous Sinusoids

Two simultaneous sinusoids are represented by the equation

$$v(t) = K_1 \cos \omega_1 t + K_2 \cos \omega_2 t. \qquad (9)$$

This signal forms a parallelogram display as shown in Fig. 6. The slopes and lengths of the parallelogram sides correspond to the frequencies and amplitudes respectively of the two signals. (Figure 6c is a photograph of the display produced by a 455 KHz sinusoid and a 200 KHz sinusoid simultaneously applied to the system.)

2. Amplitude Modulation

In the case of amplitude modulation alone, Eq. (1) becomes

$$v(t) = E(t) \cos \omega_c t. \qquad (10)$$

Since no angle modulation is present, $\alpha(t)$ in Eq. (1) is zero and θ is a constant:

$$\theta = \theta_d = \frac{\omega_c \tau}{2} + \frac{\pi}{4}. \qquad (11)$$

As will be shown, all of the displays produced by amplitude modulated signals are elongated, having maximum dimension along the

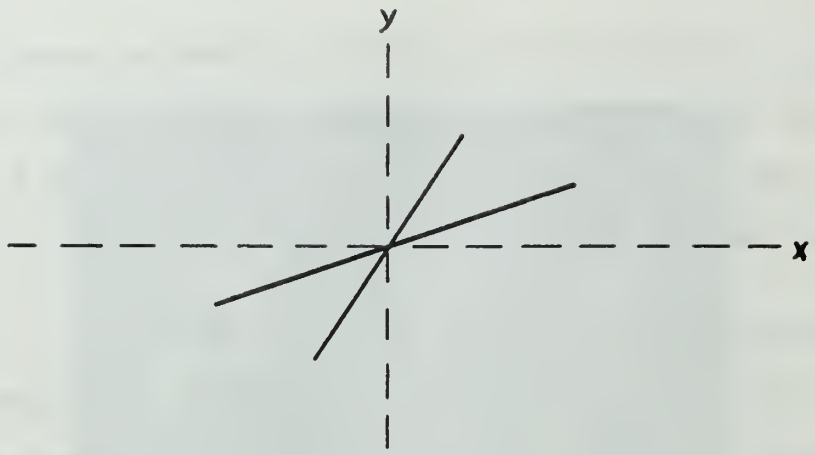

a. Diagram of the display produced by two sinusoids occurring individually.

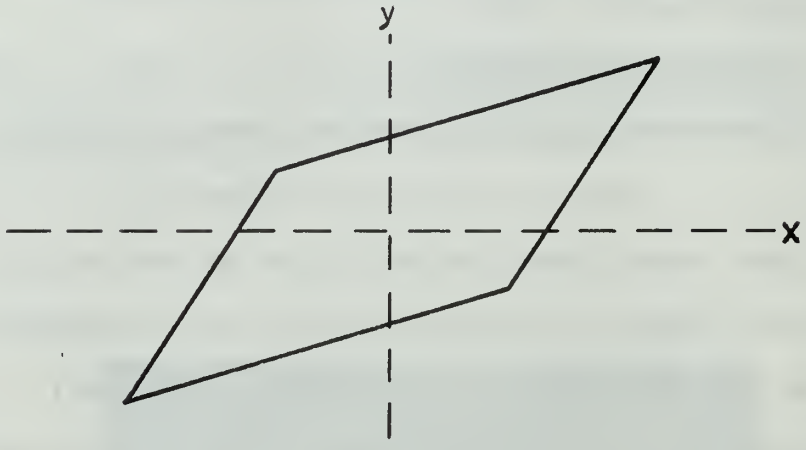

b. Diagram of the display produced by two sinusoids occurring simultaneously.

c. Photograph of the display produced by a 200 kHz and a 455 kHz sinusoid occurring simultaneously.

FIG. 6. SIMULTANEOUS SIGNAL RESPONSE OF THE LPD SYSTEM.

x' axis (θ_d radians from the horizontal). Thus in each case, carrier frequency can be determined by measuring the angle θ_d between the major axis of the display and the horizontal and using the value obtained to solve Eq. (11) for the unknown frequency, f_c.

a. Full-Carrier Amplitude Modulation

The generalized expression for full-carrier amplitude modulation by a signal f(t) is

$$v(t) = K[1 + mf(t)] \cos \omega_c t \tag{12}$$

where m is the ordinary modulation index.

(1) Amplitude Modulation by an Analog Signal. The display produced when f(t) is an analog signal is easily explained in terms of modulation by a single sinusoid. In this case, Eq. (12) becomes

$$v(t) = K[1 + m \cos \omega_m t] \cos \omega_c t \tag{13}$$

where f_m is the frequency of the modulating sinusoid. Since E(t) is now time varying rather than a constant, as in the preceding cases, the ellipse paramters a and b of Eq. (3) are functions of time. As a result, the display is formed by a time-varying ellipse. A typical ellipse formed by one RF cycle of the carrier is shown in Fig. 2. The dimensions of the major and minor axes of these ellipses vary continuously so that the ellipses may assume any form from the degenerate form of a straight line to the degenerate form of a circle. The boundary of a typical composite display is shown in Fig. 7.

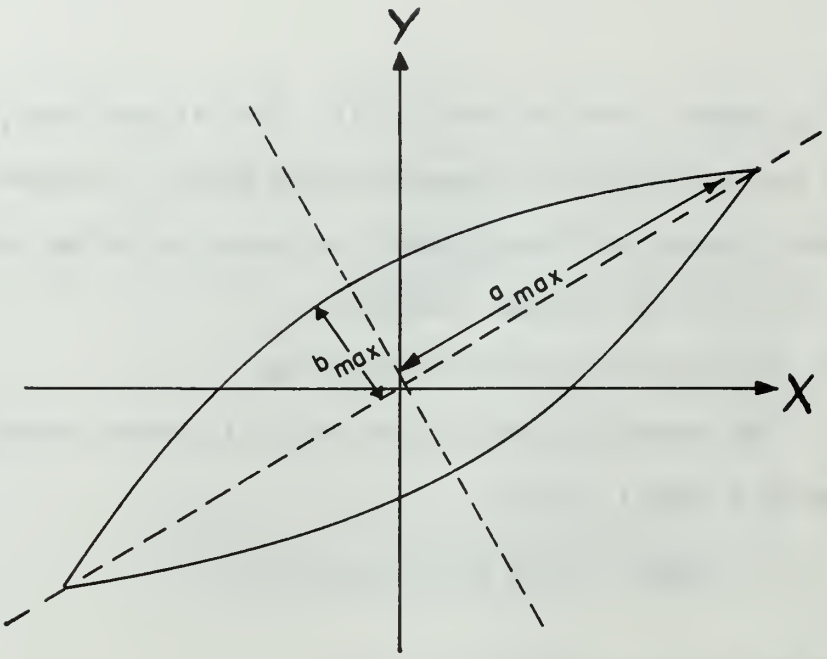

FIG. 7. BOUNDARY OF THE DISPLAY PRODUCED BY AN AM (FULL-CARRIER) SIGNAL.

The major axis of the display is rotated through an angle θ_d given by Eq. (11). Further, the width of the display can be shown to be a function of the modulation index m and modulating frequency f_m as follows for small τ.

$$b_{max} = [E(t) - E(t-\tau)]_{max} \approx \tau[\frac{dE(t)}{dt}]_{max} \quad (14)$$

$$a_{max} = [E(t) + E(t-\tau)]_{max} \approx 2E(t)_{max} \quad (15)$$

$$\frac{b_{max}}{a_{max}} \simeq \frac{\tau}{2} \frac{[\frac{dE(t)}{dt}]_{max}}{E(t)_{max}} \quad (16)$$

From Eq. 3. it can be seen that

$$[E(t)]_{max} = K(1 + m) \quad (17)$$

and

$$[\frac{dE(t)}{dt}]_{max} = Km\omega_m \, . \quad (18)$$

Therefore

$$\frac{b_{max}}{a_{max}} = (\frac{\tau}{2}) (\frac{m\omega_m}{1 + m}) \, . \quad (19)$$

a. f_m = 2 kHz, m = 0.5.

b. f_m = 2 kHz, m = 0.25.

c. f_m = 500 Hz, m = 0.5.

d. f_m = 500 Hz, m = 0.25.

FIG. 8. PHOTOGRAPHS OF THE RESPONSE OF THE LPD SYSTEM TO AN AM CARRIER. The modulating signal is a sinusoid of frequency f_m. The modulation index is m.

Figure 8 consists of photographs of the displays produced by amplitude modulation by a sinusoid. In Figs. 8a and 8b, the modulating frequency is 2 kHz. In Figs. 8c and 8d, the frequency is 500 Hz. In Figs. 8a and 8c the modulation index is .50 and in Figs. 8b and 8d the index is .25. Delay for all the above photographs is 90 μs. This series of photographs indicates the manner in which the "width" of the display is dependent upon modulating frequency and modulation index. The calculated value of $\frac{b_{max}}{a_{max}}$ in Fig. 8a using Eq. (19) is .378. The measured value is .37. Similar agreement for this type of measurement is found for all displays having measurable width.

Figure 9 is a double exposure photograph of the display produced by the signal used to obtain Fig. 8a and a like signal of half-amplitude. The photograph of Fig. 9 indicates the dependence of the size of the display on input signal amplitude.

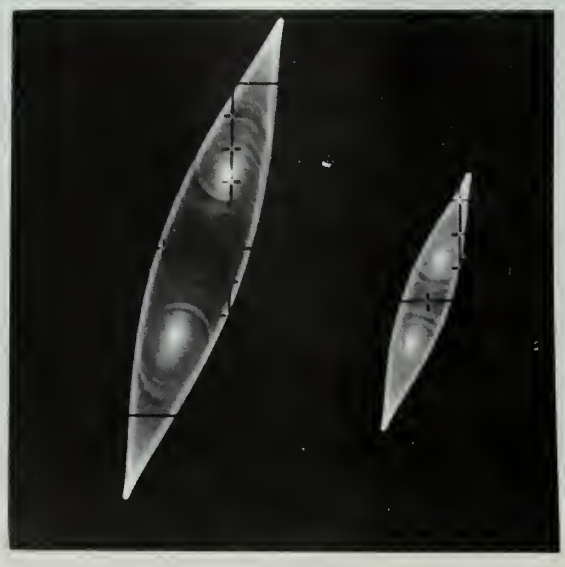

FIG. 9. SYSTEM RESPONSE TO AN AM SIGNAL AND ONE AT HALF AMPLITUDE.

For full-carrier AM by a sinusoid, the LPD system also provides an indication of the nature of the modulating signal. The two central bright spots and enhanced brightness at the vertices of the display in Fig. 8 indicate modulation by a sinusoid. The amplitude probability density function of a sinusoid is maximum at the extreme values of the sinusoid which indicates the modulating signal spends more time near its maximum and minimum values than at other levels. The bright spots in each display correspond to end points of the elliptical display formed when the carrier is near its maximum and minimum levels.

(2) Continuous Wave, (On-Off Keying). Continuous-wave(CW) signals have the form

$$v(t) = K\, S(t) \cos \omega_c t \tag{20}$$

where S(t) is the switching function and takes on the values 0 or 1. The resultant signal is simply a pulsed sinusoid. Signals of this type include certain radar signals as well as the common CW communication transmissions.

When a sinusoidal signal is present at one input port of the QHJ and no signal is present at the other port, the output signals are, at one port, the input sinusoid, and at the other port, the input sinusoid phase shifted by $-\frac{\pi}{2}$. The resultant display is a circle. The delay line in one of the signal channels of the system insures that, for pulsed RF signals, this single-input condition occurs twice each RF pulse. That is, for τ seconds after the pulse appears at the input to the system, and for τ seconds after the input pulse has ceased, there is a signal into but one port of the QHJ. During each of these τ second intervals, a circle is formed on the CRT screen.

If the pulse duration is greater than τ seconds, the period of time from τ seconds after the initiation of the pulse until the pulse ceases results in a steady-state display. In the case of rectangular pulses having no intrapulse modulation, the steady-state portion of the display is a straight line as described in the case of a single sinusoid.

The composite display is, therefore, a circle with a line through it as shown in Fig. 5. This is an easily recognizable display indicating the presence of pulsed or digital modulation. Carrier frequency is determined as before by the angle from the horizontal of the straight line trace.

If the pulse width is less than the system delay, there will be no steady-state display; that is, the straight line trace will not exist. These results suggest a simple method of measuring pulse width. If the system delay is increased until the straight line trace just disappears, the delay line setting should approximate the pulse width. This procedure is demonstrated in Fig. 10. The signal is an RF pulse with duration of 90 μs, and a repetition rate of about 550 Hz. System delay in the composite photograph, Fig. 10b, is from left to right, 50 μs, 78 μs, 86 μs, and 90 μs. With the delay set at 90 μs, the straight line trace disappears as predicted.

(3) Pulse Amplitude Modulation. In the case of carrier amplitude modulation by a train of amplitude-modulated pulses (PAM-AM), the display produced by each pulse is like that produced by on-off keying. However, since a number of different pulse levels may be transmitted, the composite display is the superposition of concentric displays as shown in Fig. 11a. Each circle (transient-portion of the

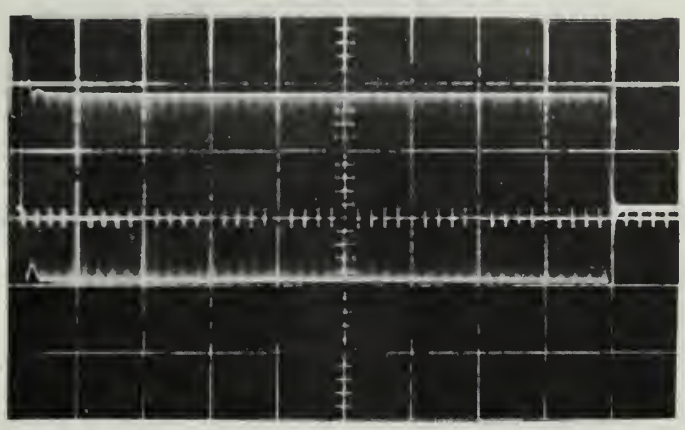

a. Time waveform; pulse width is 90 μs.

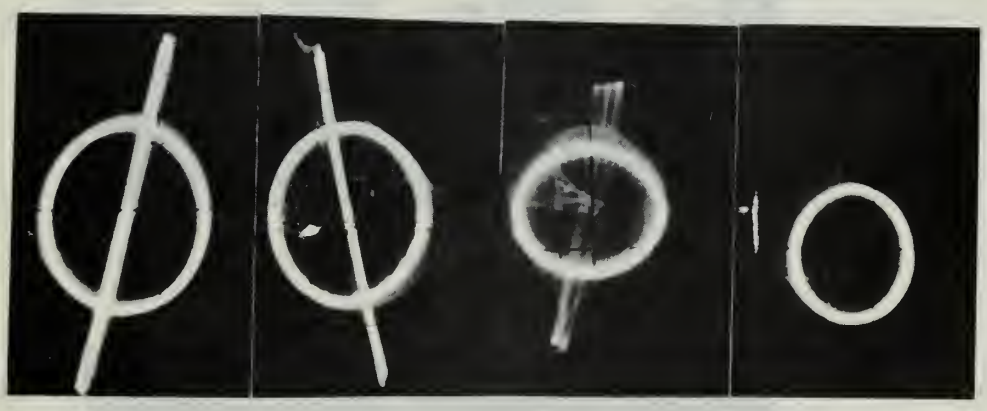

b. Typical displays; from left to right, the value τ of system delay is 50 μs, 78 μs, 86 μs, and 90 μs.

FIG. 10. PHOTOGRAPHS OF THE RESPONSE OF THE LPD SYSTEM TO A PULSED SIGNAL.

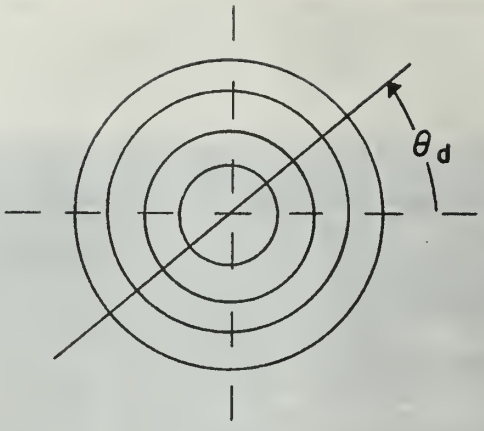

a. Diagram of the response to a four-level signal.

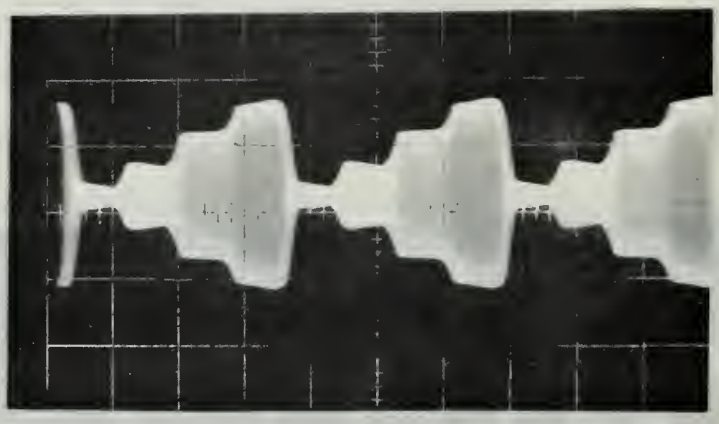

b. Time waveform of a PAM-AM signal.

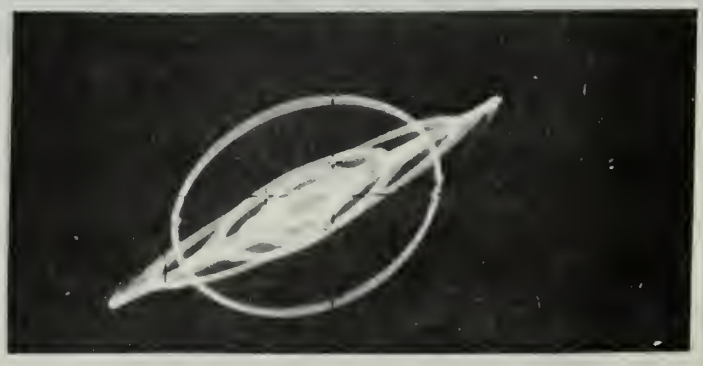

c. Display corresponding to b.

FIG. 11. RESPONSE OF THE LPD SYSTEM TO A PAM-AM SIGNAL.

display), corresponds to one of the amplitude levels transmitted. This display, therefore, provides a measure of the number of levels of the modulating signal.

Figure 11c is a photograph of the display produced by the signal whose time wave form is indicated in Fig. 11b. This is not a true PAM-AM signal because, although four discrete levels are transmitted, the carrier is not pulsed on and off; at no time does the modulation equal zero. The various ellipses correspond to the transient portion of the display and indicate one level of signal at one port of the QHJ and a different level at the other port.

b. Double-Sideband Suppressed Carrier

The display formed by a double-sideband, suppressed-carrier amplitude-modulated signal is readily explained by first considering modulation by a sinusoid. The modulated carrier has the form

$$v(t) = K \cos \omega_m t \cos \omega_c t. \tag{21}$$

This equation reduces to the sum and difference frequency form

$$v(t) = \frac{K}{2} \cos(\omega_c+\omega_m)t + \frac{K}{2} \cos(\omega_c-\omega_m)t. \tag{22}$$

The display for this signal is identical to the display for two simultaneous sinusoids (Fig. 6). An example is shown as Fig. 12a.

When the modulating signal is complex, such as a voice signal, many different frequency components are present. The resultant display appears as in Fig. 12b. Here again a distinctive display is obtained. The carrier frequency is determined by the orientation of the major axis of the display.

The distinct, star-like pattern in the center of the display is caused by the instantaneous ellipses degenerating to

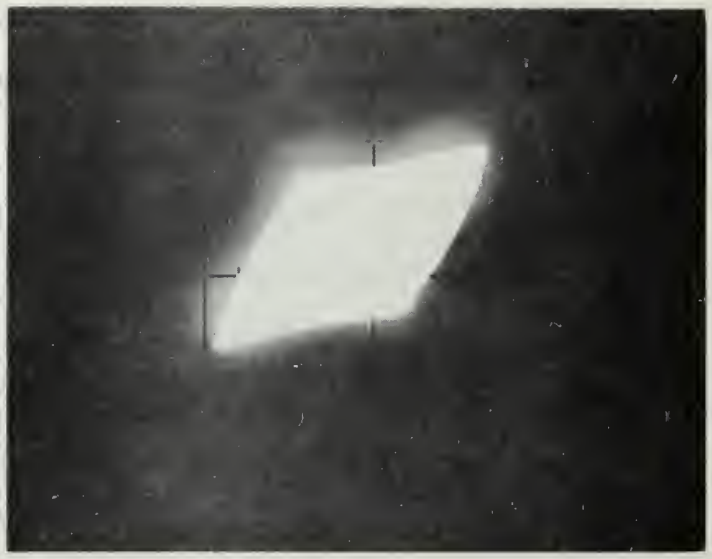

a. Modulation by a 2 kHz sinusoid.

b. Modulation by a voice signal.

FIG. 12. PHOTOGRAPHS OF THE RESPONSE OF THE LPD SYSTEM TO DOUBLE-SIDEBAND SUPPRESSED-CARRIER AM SIGNALS.

straight line traces along each axis. That is, at various instants of time, either a or b in Eq. (3) is equal to zero.

c. Single-Sideband

It has been shown that a single-sideband (SSB) signal can be expressed as [Ref. 4]

$$v(t) = E(t) \cos [\omega_c t + \alpha(t)]. \tag{23}$$

In particular, if $E_m(t)$ is the actual function to be transmitted, and $\sigma(t)$ is the Hilbert Transform of $E_m(t)$, then the signal is given by

$$v(t) = \{[E_m(t)]^2 + \sigma^2(t)\}^{1/2} \cos [\omega_c t + \arctan \frac{\sigma(t)}{E_m(t)}] \tag{24}$$

This is a signal involving suppressed-carrier amplitude modulation and angle modulation.

The resultant display might be explained as a double-sideband, suppressed-carrier display, (from the amplitude modulation term in Eq. (24)), which wobbles due to the carrier angle modulation. This display is noiselike in appearance and is probably the least distinguishable of all the displays investigated. The display does possess a rippling, watery-like character which is an aid to recognition and is evident in one of the movie sequences but does not appear in a still photograph.

Figure 13a is a photograph of a single-sideband voice transmission taken directly from the IF strip of an R-390A receiver. Carrier frequency is 14.322 MHz. Figure 13b is a photograph of the central part of the same type of display much enlarged. One nearly perfect parallelogram is faintly discernible in this photograph, but in general, neither photograph is uniquely distinctive.

a. Typical display.

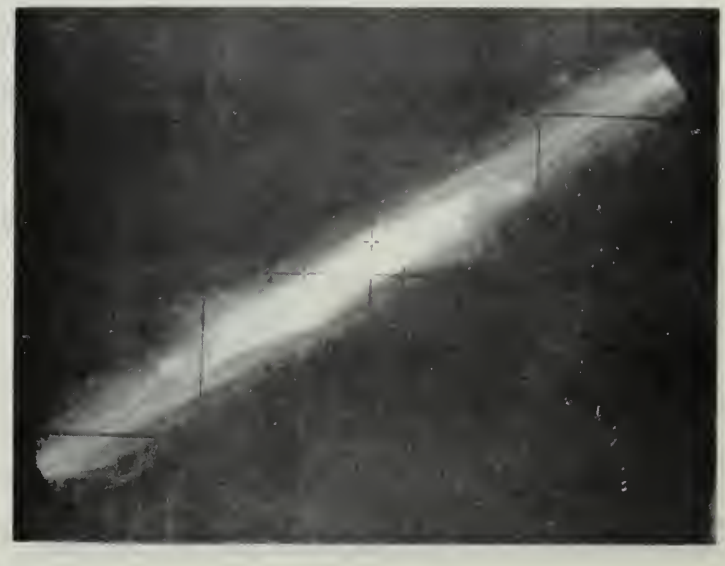

b. Enlarged central portion of a.

FIG. 13. PHOTOGRAPHS OF THE RESPONSE OF THE LPD SYSTEM TO SINGLE-SIDEBAND AM SIGNALS. The modulating signal is voice.

3. Angle Modulation

In the case of angle modulation, the envelope E(t) is constant but the phase angle $\alpha(t)$ is a function of time. The signal in this case can be expressed as

$$v(t) = K \cos[\omega_c t + \alpha(t)]. \tag{25}$$

Because of the absence of amplitude modulation, the elliptical parameter b in Eq. (5) is zero, and the instantaneous ellipse degenerates to a straight line.

If τ is sufficiently small,

$$\frac{\alpha(t) - \alpha(t - \tau)}{2} \approx \frac{\tau}{2} \frac{d\alpha(t)}{dt} . \tag{26}$$

but

$$\omega_c + \frac{d\alpha(t)}{dt} = \omega_i(t). \tag{27}$$

therefore Eq. (2) becomes

$$\theta \approx \frac{\tau}{2} \omega_i(t) + \frac{\pi}{4} \tag{28}$$

and θ is seen to be a linear function of the instantaneous carrier frequency for small values of τ.

The resultant display is contained within a region the outline of which is shown in Fig. 14. The intensity distribution within this region is dependent upon the statistics of the instantaneous frequency and indicates whether the modulating function is analog or digital as suggested in the following discussion.

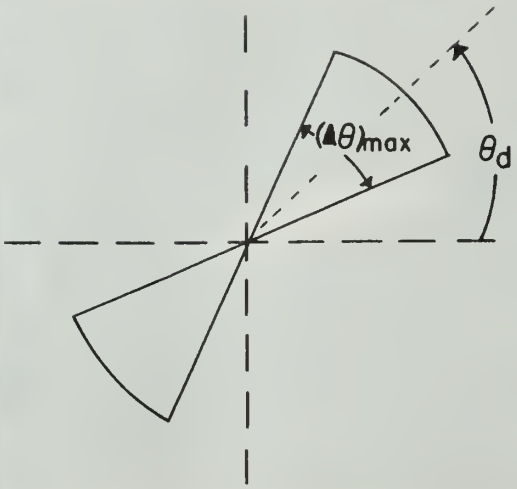

FIG. 14. DIAGRAM OF THE RESPONSE OF THE LPD SYSTEM TO AN ANGLE-MODULATED CARRIER.

Average carrier frequency can be determined by measuring the angle from the horizontal to the central axis of the display. A relative measure of signal strength is given by the size of the display. The peak radian frequency deviation, $(\Delta\omega)_{max}$ of the carrier is related to the peak angular deviation $(\Delta\theta)_{max}$ of the display from θ_d:

$$(\Delta\omega)_{max} = \frac{2\ (\Delta\theta)_{max}}{\tau} . \qquad (29)$$

a. Angle Modulation by an Analog Signal

The display produced when $\alpha(t)$ is an analog signal is easily explained in terms of modulation by a single sinusoid. In this case Eq. (25) becomes

$$v(t) = K \cos[\omega_c t + k_p A \cos \omega_m t] \qquad (30)$$

where k_p is a property of the modulator, and converts volts of the

modulating signal to radians of angle of the carrier. The display appears as predicted above, indicating average carrier frequency, peak frequency deviation, and a relative measure of signal strength.

Figure 15 consists of photographs of the display resulting from frequency modulation by a 2 kHz sinusoid. The peak-to-peak frequency deviation is 5 kHz for Figs. 15a and 15b and 10 kHz for Figs. 15c and 15d. System delay is 90 μs for Figs. 15a and 15c and 40 μs for Figs. 15b and 15d. These photographs demonstrate the dependence of $(\Delta\theta)_{max}$ on system delay and peak frequency deviation.

The theoretical value for $(\Delta\theta)_{max}$ in Fig. 15b computed using Eq. (29) was .63 radians. The measured value was .655 radians. Similar agreement was obtained in the other cases.

Again, the nature of the modulating signal is apparent. In all the photographs, the display is brightest at the borders, indicating that the instantaneous frequency dwells near maximum deviation from the carrier frequency. This condition suggests that a sinusoid is used as the modulating function.

b. Angle Modulation by a Digital Signal

(1) Steady-State Analysis.

(a) Frequency-Shift Keying (FSK). Frequency modulation by a digital signal results in a carrier having discrete frequencies corresponding to the discrete levels of the modulating signal. These FSK carriers generate a distinct display.

This type of signal is expressed as

$$v(t) = K \cos \{[\omega_c + k_f d(t)(\Delta\omega)]t\} \qquad (31)$$

where d(t) is the modulating data and $k_f d(t)$ takes on integral values 0,1,2,... corresponding to the discrete levels of d(t). Here k_f is a

a. $2(\Delta f)_{max}$ = 5 kHz
τ = 90 μs.

b. $2(\Delta f)_{max}$ = 5 kHz
τ = 40 μs.

c. $2(\Delta f)_{max}$ = 10 kHz
τ = 90 μs.

d. $2(\Delta f)_{max}$ = 10 kHz
τ = 40 μs.

FIG. 15. PHOTOGRAPHS OF THE RESPONSE OF THE LPD SYSTEM TO A FM CARRIER. The modulating signal is a 2 kHz sinusoid. The peak-to-peak frequency deviation is $2(\Delta f)_{max}$. System delay has value τ.

property of the modulator, and converts volts of d(t) to radians per second of frequency. In the most-common modulating signal format, $k_f d(t)$ is either 0 or 1 (binary data). If the carrier instantaneous frequency remains constant for periods of time long with respect to τ, then in general the display consists of a collection of straight line traces. Each line corresponds to a discrete frequency transmitted.

Each discrete frequency is directly measureable as in the case of a single sinusoid. Relative amplitudes are again preserved and, thus, frequency-selective fading is easily recognized. In addition, if one or more of the carrier frequencies predominates (greater duty factor) in a particular signal format, the display will indicate this condition by enhanced brightness of the corresponding trace.

Figure 16a is the display produced by frequency modulation by a symmetrical 500 Hz square wave. The time wave-form of the modulating signal appears in Fig. 16b. Figure 16c is the display produced when the modulation is nonsymmetrical as in Fig. 16d. The higher frequency in this case is dominant, and this fact is evident from the display.

(b) Phase-Shift Keying (PSK). Phase modulation by a digital signal results in a carrier having discrete phases corresponding to the discrete levels of the modulating signal. These PSK carriers also generate a distinct display.

A phase-shift-keyed signal is expressed as

$$v(t) = K \cos[\omega_c t + k_p d(t)(\Delta\phi)] \tag{32}$$

where d(t) as before is the modulating data and $k_p d(t)$ takes on

a. Display corresponding to b.

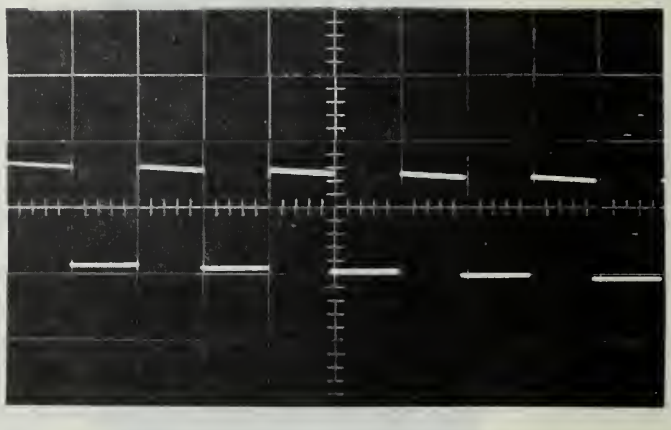

b. Time waveform of the symmetrical 500 Hz square-wave modulating voltage.

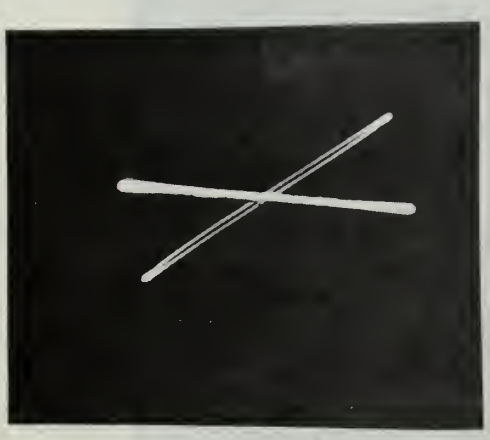

c. Display corresponding to d.

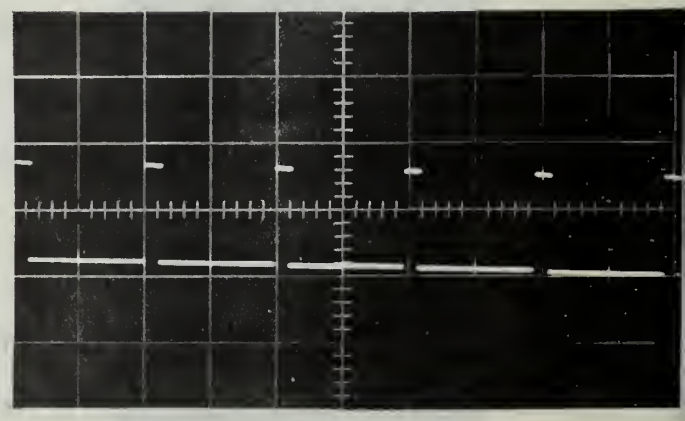

d. Time waveform of the nonsymmetrical 500 Hz square-wave modulating voltage.

FIG. 16. PHOTOGRAPHS OF THE RESPONSE OF THE LPD SYSTEM TO FSK SIGNALS.

integral values 0, 1, 2, ... corresponding to the discrete levels of d(t). Here k_p is a property of the modulator and converts volts of d(t) to radians of phase.

In the case of binary data (two-level modulating signal), $k_p d(t)$ is 0 or 1 and so from Eq. (23)

$$\alpha(t) - \alpha(t - \tau) = 0 \text{ or } \pm \Delta\phi \tag{33}$$

Therefore, θ has three possible values

$$\theta = \frac{\omega_c \tau}{2} + \frac{\pi}{4} = \theta_d \tag{34}$$

$$\theta = \frac{\omega_c \tau}{2} + \frac{\pi}{4} + \frac{\Delta\phi}{2} \tag{35}$$

$$\theta = \frac{\omega_c \tau}{2} + \frac{\pi}{4} - \frac{\Delta\phi}{2} . \tag{36}$$

The resultant display appears as in Fig. 17a.

The heavy, central trace is at an angle θ_d as given by Eq. (34). Carrier frequency can again be determined by measuring this angle.

The angle θ is given by Eq. (35) or Eq. (36) only for τ seconds after d(t) changes values. As a result, the peripheral traces are less dense than the central trace. Note that the value $\frac{\Delta\phi}{2}$ is measureable directly from the display and this measurement is independent of the value of τ.

The display produced is unique, indicates a phase-keyed signal, and provides a means for determining carrier frequency, amount of phase shift, and a relative measure of signal strength. Figure 17b is a family of displays produced by phase-shift keying by a 1250 Hz square wave. Amounts of phase shift are, from left to right, 24^o, 106^o, and 170^o.

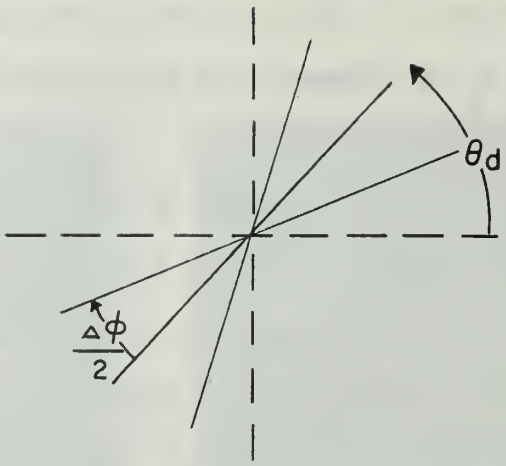

a. Diagram of the response to bi-phase modulation.

b. Typical displays; from left to right, the value of carrier phase shift is 24°, 106° and 170°.

FIG. 17. RESPONSE OF THE LPD SYSTEM TO PSK SIGNALS.

(2) Transient Analysis.

(a) Frequency-Shift Keying (FSK). The display produced by FSK when the signal data rate is low with respect to the system delay has been considered previously. If the instantaneous frequency remains constant for periods of time large with respect to τ, the display can be thought of as formed by a number of discrete sinusoids occurring individually. However, Fig. 16a and 16c exhibit a faint but continuous intensity distribution between the two straight line traces indicating that the trace does not change its orientation abruptly, but does so in a continuous manner. This section is concerned with the manner in which this transition occurs and the effects that the relation between system delay and data rate have upon the transition.

Consider frequency modulation by a symmetrical square wave. The instantaneous frequency of such a signal appears as in Fig. 18a. Here $\frac{T_p}{2}$ is the square wave half period or pulse width. The phase modulation $\alpha(t)$ which occurs as a result of the changes in instantaneous frequency appears as in Fig. 18b. During t_1 the instantaneous frequency is greater than ω_c and $\alpha(t)$ increases linearly with time at a rate equal to $\Delta\omega$. During t_2, the instantaneous frequency is less than ω_c and $\alpha(t)$ decreases in the same manner. If the modulating wave form is symmetrical, no net phase modulation occurs in the interval t_1 and t_2.

Case 1: $\frac{T_p}{2} > \tau$

When $\frac{T_p}{2}$ the half period of the square wave (the dwell time of the signal at a fixed frequency), is greater than

the system delay, $\alpha(t)$ and $\alpha(t - \tau)$ appear as shown in Fig. 18c. It follows that θ_d has the form shown in Fig. 18d. This corresponds to the normal display as shown in Fig. 16a. The transition period occurs for τ seconds after the instantaneous frequency changes values. The change in trace orientation is seen to be a linear function of time.

Case 2: $\frac{T_p}{2} = \tau$

If the square wave half period exactly equals the system delay, $\alpha(t)$ and $\alpha(t - \tau)$ appear as in Fig. 19a and the resultant angle θ_d as in Fig. 19b. In this case θ does not have a static value, and the display does not have distinct boundaries, but it will look like the display for frequency modulation by a continuous signal. This phenomenon provides a method of determining the approximate data rate of an unknown signal by adjustment of the system delay until the above condition is attained.

Case 3: $\frac{T_p}{2} < \tau$

In the case of signals with extremely high data rates, $\alpha(t)$ and $\alpha(t - \tau)$ may appear as indicated in Fig. 19c and the resultant angle, θ as in Fig. 19d. This is similar to Case 1 and it follows that the resultant display will always have intense boundaries; that is, θ will remain constant during certain intervals if and only if $\tau \neq \frac{nT_p}{2}$ where n is an integer.

Further, for symmetrical square-wave modulation and $\frac{T_p}{2} < \tau$, $\Delta\theta$ does not depend only upon τ and $\Delta\omega$ but also upon the relationship between τ and $\frac{T_p}{2}$. Here, $\Delta\theta$ is the deviation of θ

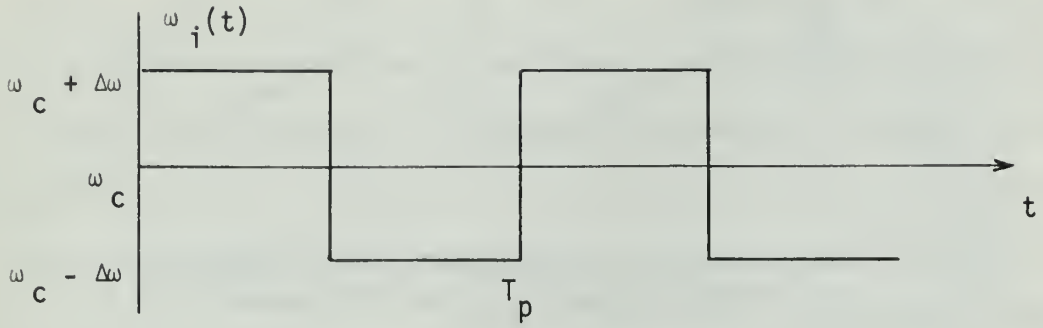

a. Instantaneous frequency of the carrier.

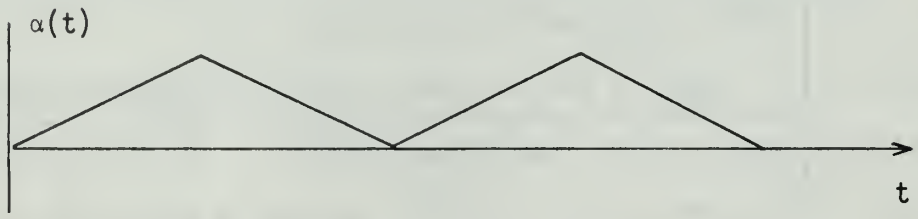

b. Phase deviation of the carrier.

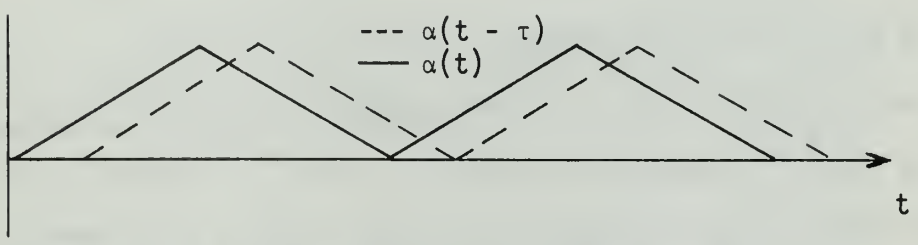

c. Phase deviation of the carrier in the delayed and undelayed channels of the LPD system.

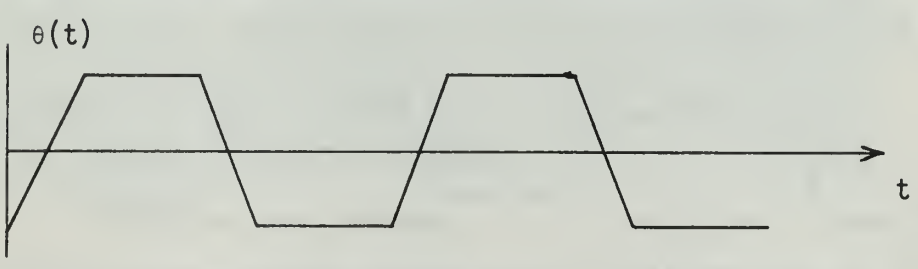

d. Resultant display angle.

FIG. 18. TRANSIENT RESPONSE OF THE LPD SYSTEM TO FSK SIGNALS. The period T_p of the modulating signal is greater than twice the value τ of system delay.

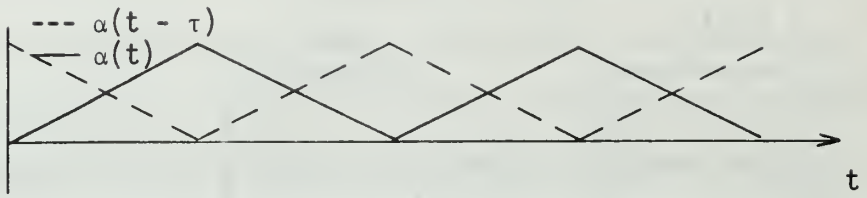

a. Phase deviation of the carrier in the delayed and undelayed channels of the LPD system; $T_p/2 = \tau$.

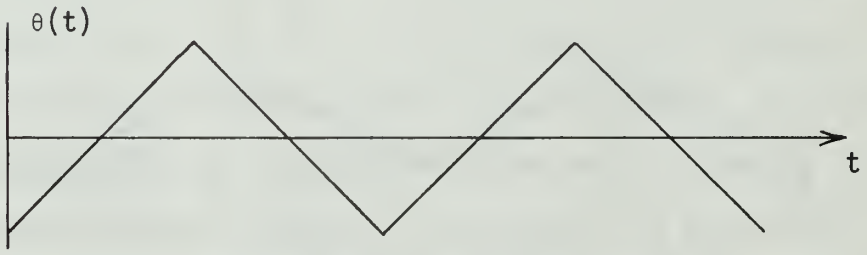

b. Resultant display angle; $T_p/2 = \tau$.

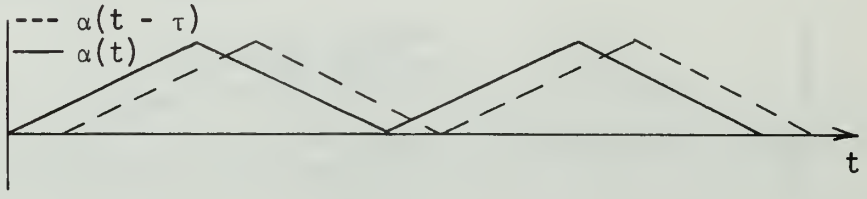

c. Phase deviation of the carrier in the delayed and undelayed channels of the LPD system; $T_p/2 < \tau$.

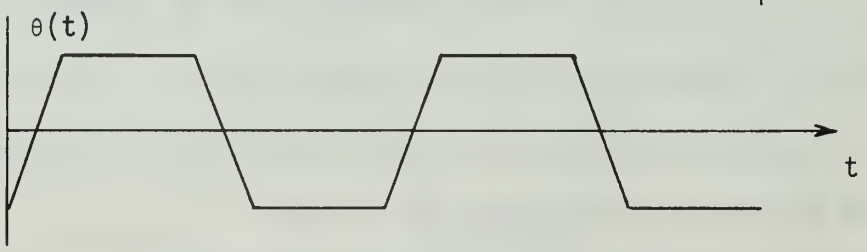

d. Resultant display angle; $T_p/2 < \tau$.

FIG. 19. TRANSIENT RESPONSE OF THE LPD SYSTEM TO FSK SIGNALS. The period T_p of the modulating signal is less than or equal to twice the value τ of system delay.

from θ_d. For $\tau = (2n + 1)\frac{T_p}{2}$, $\Delta\theta$ is a maximum and for $\tau = nT_p$, $\Delta\theta$ is a minimum. That is, when the system delay is equal to an integral number of whole periods of the modulating waveform, no difference in phase modulation is apparent. In this case $\alpha(t)$ equals $\alpha(t-\tau)$ and the resultant display is a straight line trace where $\theta = \theta_d = \frac{\omega_c \tau}{2} + \frac{\pi}{4}$.

Figure 20 comprises a photographic study of the transient effects just presented. Modulation is by a symmetrical square wave with $\frac{T_p}{2}$ = 30 μs.

Note that, as predicted, there is no evidence of enhanced brightness at the borders of the displays in Fig. 20a where $\tau \simeq \frac{3T_p}{2}$ and $\tau \approx \frac{T_p}{2}$. Bright edges appear on all of the displays in Fig. 20b indicating a constant value of θ for an interval of time. As stated above $(\Delta\theta)_{max}$ is no longer a linear function of τ in this case. Finally, $(\Delta\theta)_{min}$ is a minimum for τ = 58 μs, as predicted.

(b) Phase-Shift keying (PSK). If, as in the case of a phase-shift-keyed signal, the phase shift occurs in zero time, the straight line trace also changes orientation in zero time. This phenomenon can be explained if the change in phase is considered as the result of an infinite change in frequency which occurs in zero time. The transient analysis then follows as in the case of FSK where in each case, the rate of change of θ is equal to $\Delta\omega$.

c. Pulsed Frequency Modulation

If the carrier frequency of a pulsed signal is modulated, a unique display is produced. Such a signal can be expressed as

$$v(t) = K\, S(t) \cos [\omega_c t + \alpha(t)] \qquad (37)$$

where S(t) is the switching function and takes on values 0 or 1 and $\alpha(t)$ denotes the angle modulation which occurs during the pulse.

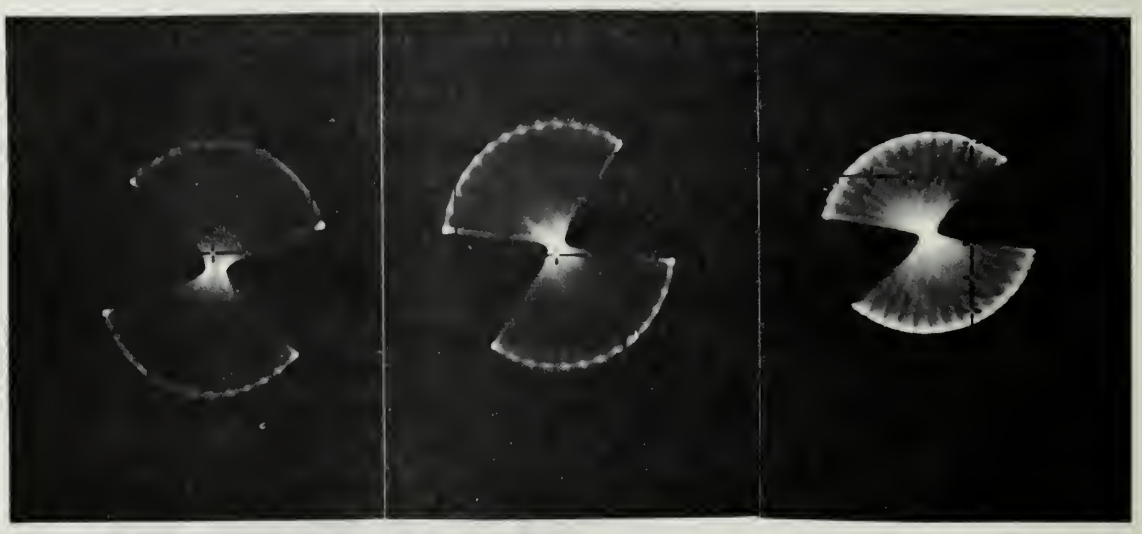

τ = 28 μs	τ = 32 μs	τ = 90 μs
$2\tau/T_p$ = 0.93	$2\tau/T_p$ = 1.07	$2\tau/T_p$ = 3.00

a. Display edges not enhanced.

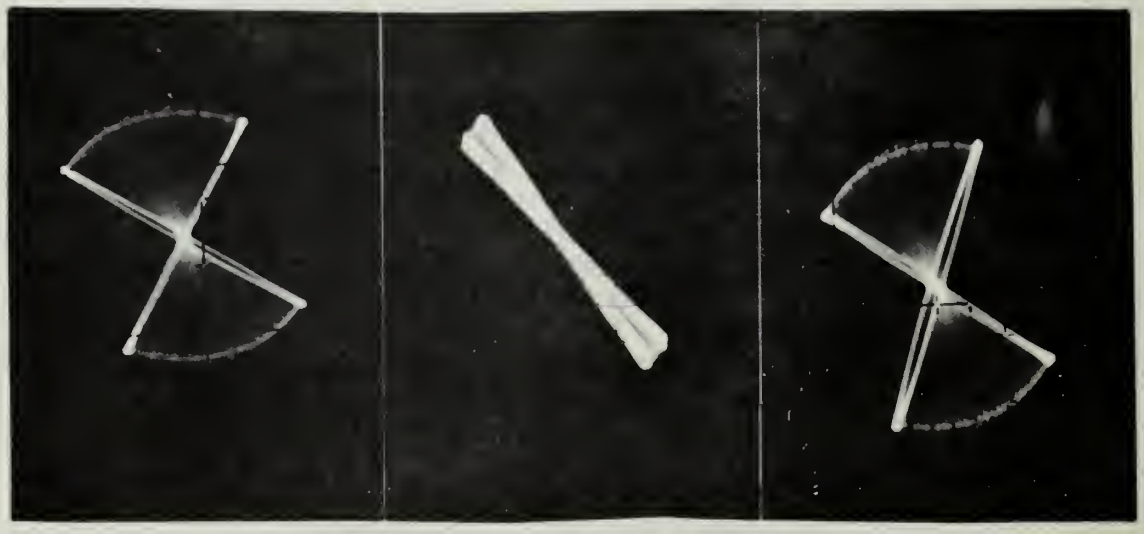

τ = 20 μs	τ = 58 μs	τ = 78 μs
$2\tau/T_p$ = 0.67	$2\tau/T_p$ = 1.93	$2\tau/T_p$ = 2.60

b. Display edges enhanced.

FIG. 20. PHOTOGRAPHIC STUDY OF THE TRANSIENT RESPONSE OF THE LPD SYSTEM TO FSK SIGNALS. T_p is the period of the square-wave modulating voltage. System delay has value τ.

An example of intentional intrapulse FM is a rectangular pulse whose carrier frequency increases linearly with time for the duration of the pulse. This type of signal is known as a "chirp" pulse and has applications in pulse compression systems (radar, sonar, frequency-measuring devices).

Figure 21 is a photograph of the system display produced by a "chirp" pulse of duration .2 milliseconds and pulse repetition rate 715 Hz. During the pulse, the carrier frequency is swept linearly over a 4 kHz band. The display exhibits the circular trace which is characteristic of a pulsed signal and the fan-like trace which is characteristic of frequency modulation. Average carrier frequency is determined as before by measuring the angle from the horizontal to the central axis of the display.

4. Autocorrelation Function of a Gaussian Process

It has been shown that the normalized autocorrelation function $\bar{\rho}(\tau) = \frac{R_{nn}(\tau)}{R_{nn}(0)}$ of a narrowband gaussian process n(t) can be determined from the parameters of the LPD system display generated by this random excitation [Ref. 1, p. 124]. The equation relating the autocorrelation function and display parameters is

$$\bar{\rho}(\tau) = \frac{a^2 - b^2}{a^2 + b^2} \sin 2\theta_d \tag{38}$$

where as before

$$\theta_d = \frac{\omega_o \tau}{2} + \frac{\pi}{4} \tag{39}$$

and a and b are the standard ellipse parameters measurable from the display, ω_o is the center radian frequency of the narrowband process, and τ is the system delay.

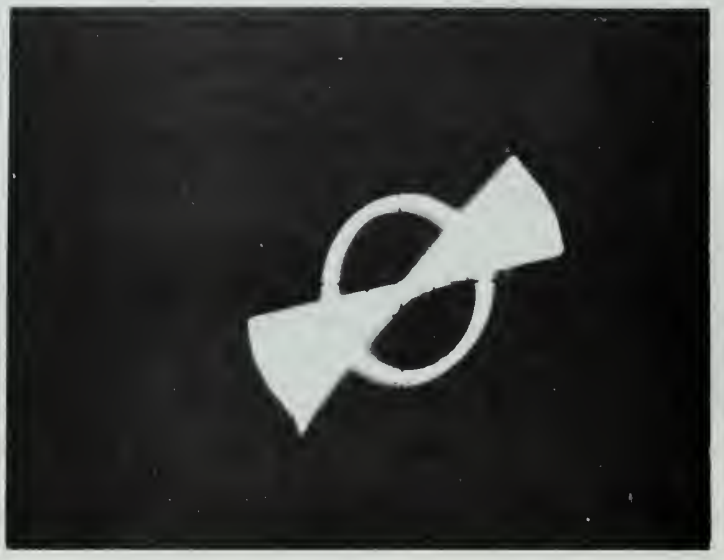

FIG. 21. PHOTOGRAPH OF THE RESPONSE OF THE LPD SYSTEM TO A RECTANGULAR PULSE WITH INTRAPULSE LINEAR FM.

From Eq. (28), when $|\overline{\rho}(\tau)| = 1$, (condition of perfect correlation), a = 0 or b = 0 and the display is a straight line. When $|\overline{\rho}(\tau)| = 0$ (no correlation), b = a and the display is circular.

Rectangular bandpass gaussian noise having a bandwidth of 50 kHz and centered at 500 kHz was investigated. The autocorrelation function and power spectral density are Fourier transform pairs as demonstrated in Fig. 22a for a lowpass process. The autocorrelation function $\overline{\rho}(\tau) = \frac{\sin \omega_c \tau}{\omega_c \tau}$ has its first zero crossing at $\tau = \frac{1}{2f_c}$.

When the process is bandpass,

$$\overline{\rho}(\tau) = \frac{\sin \omega_c \tau}{\omega_c \tau} \cos \omega_o \tau \, . \tag{40}$$

The $\cos \omega_o \tau$ term imparts a fine structure to the $\frac{\sin \omega_c \tau}{\omega_c \tau}$ envelope as shown in Fig. 22b.

Values for the normalized autocorrelation function of Eq. (38) were determined with delay settings from 0 to 20 μs in 4 μs increments. Since the center frequency f_o is 500 kHz and since data were taken at 4 μs increments, the fine structure mentioned above is not observed because $\cos \omega_o \tau = 1$ for every data point. Further, θ_d in Eq. (38) is always equal to $\frac{\pi}{4}$; hence, the $\sin 2\theta_d$ term in Eq. (37) equals unity in all cases.

Photographs of the resultant displays are included as Fig. 23. A plot of the experimental and theoretical values for the normalized autocorrelation function appears as Fig. 24. Good agreement is indicated.

B. SIGNAL MONITORING

As stated in the introduction, one of the goals of this project was to monitor live signals in the HF band. These signals were taken

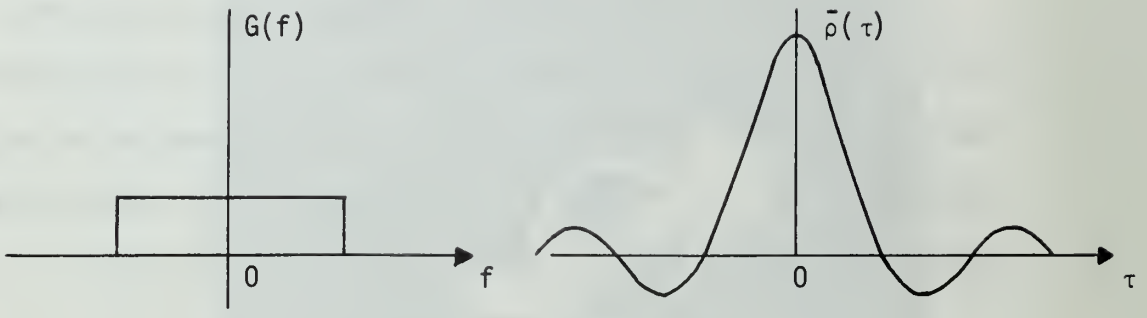

a. Lowpass process.

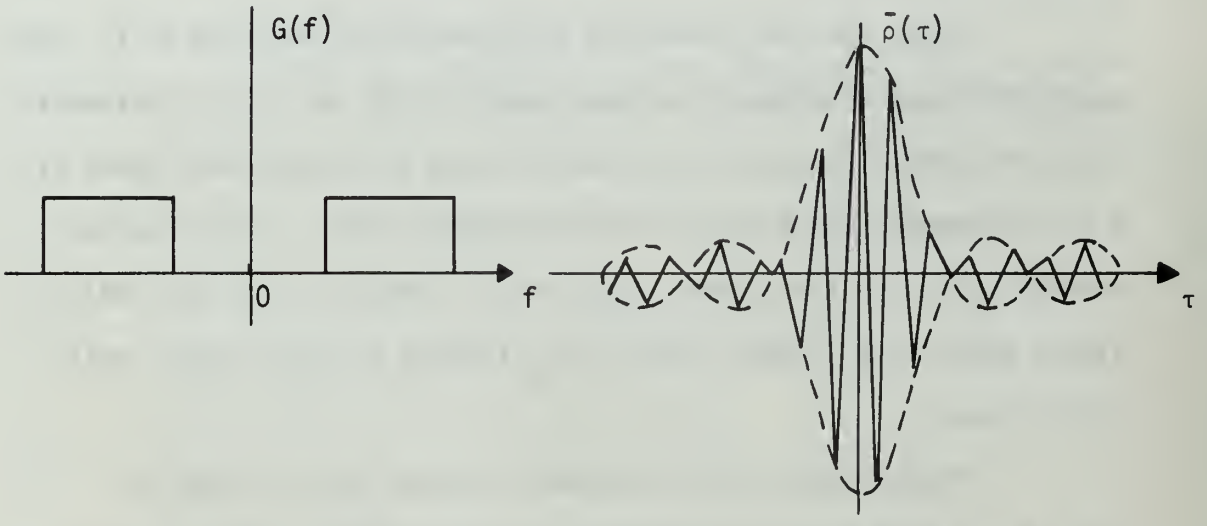

b. Bandpass process.

FIG. 22. POWER SPECTRAL DENSITY G(f) AND NORMALIZED AUTOCORRELATION $\bar{\rho}(\tau)$ FUNCTIONS FOR RANDOM PROCESSES.

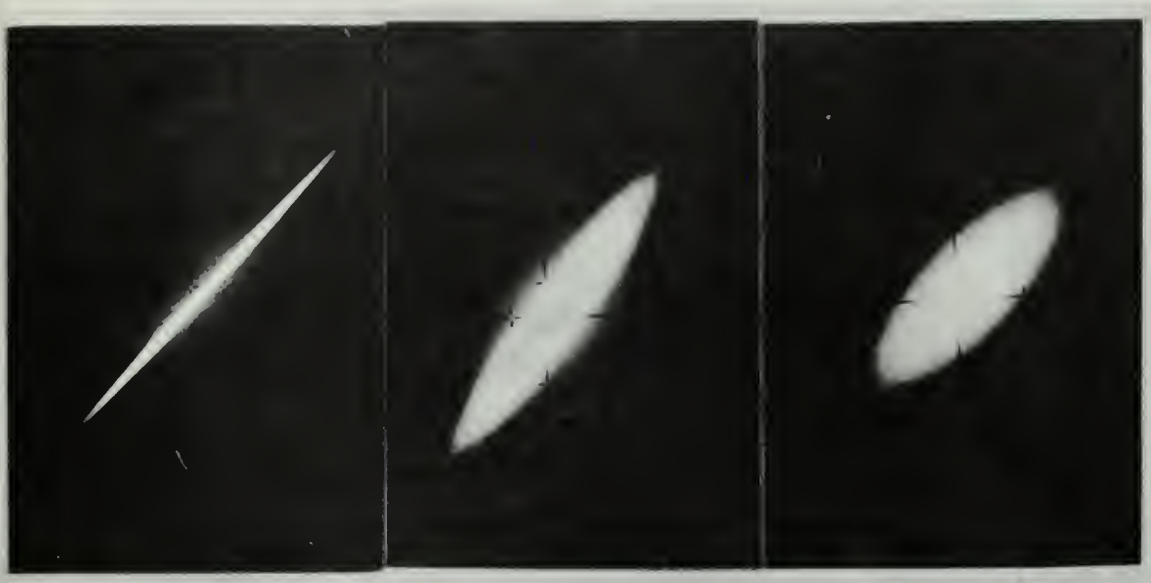

τ = 0 μs τ = 4 μs τ = 8 μs

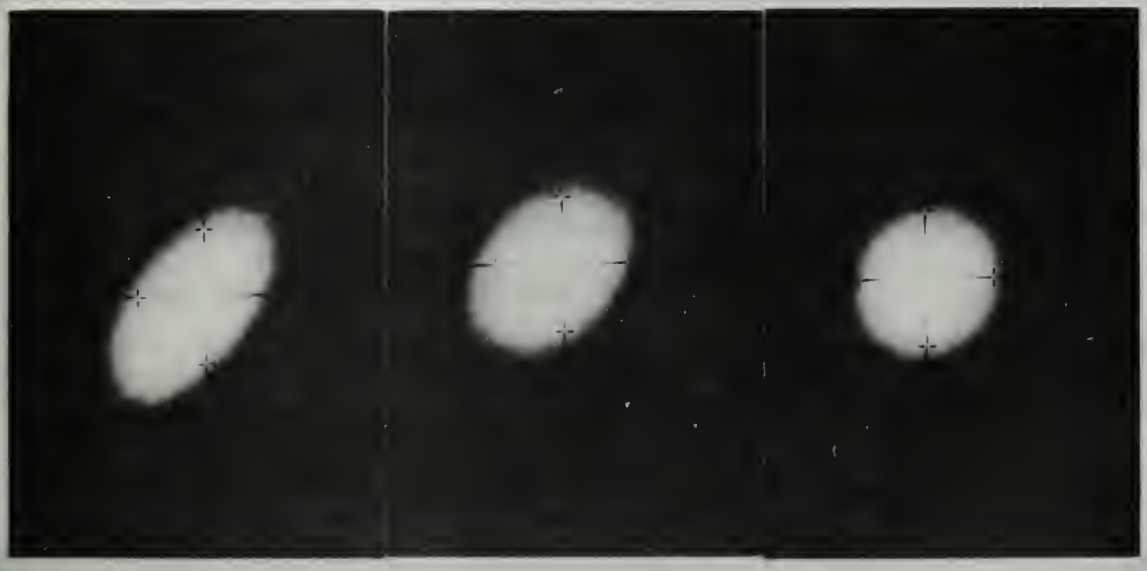

τ = 12 μs τ = 16 μs τ = 20 μs

FIG. 23. PHOTOGRAPHS OF THE RESPONSE OF THE LPD SYSTEM TO BANDPASS GAUSSIAN NOISE.

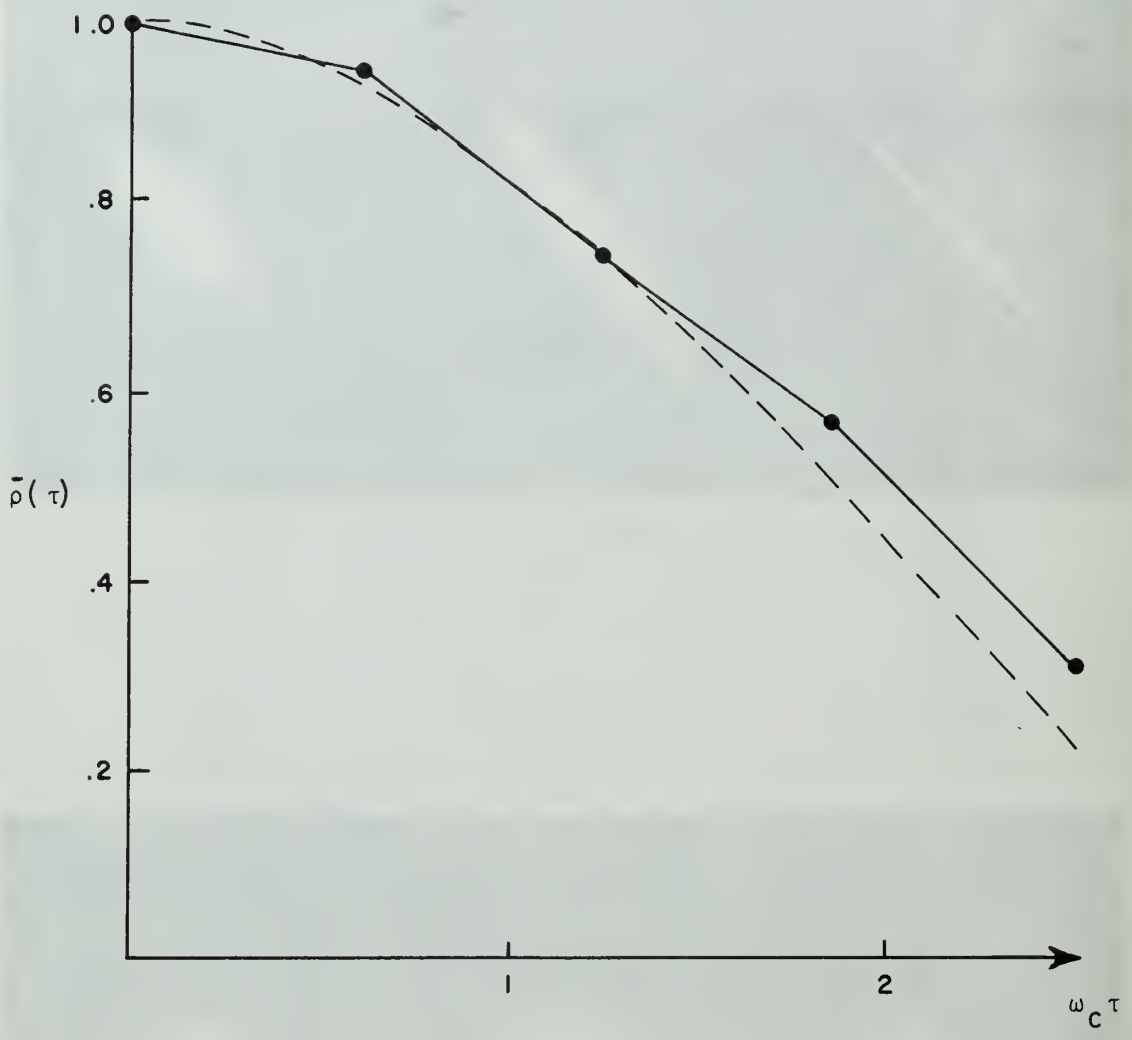

FIG. 24. A COMPARISON OF THE THEORETICAL AND EXPERIMENTAL VALUES OF THE AUTOCORRELATION FUNCTION OF BANDPASS GAUSSIAN NOISE.

directly from the IF strip of an R-390A receiver and were applied directly to the system. The resultant displays were photographed with an 8mm movie camera. The film strip in its final form is approximately 12 minutes long and contains examples of:

(1) standard broadcast AM
(2) double-sideband suppressed carrier AM
(3) single-sideband AM
(4) continuous wave, on-off keying
(5) frequency-shift keying.

The following results are of particular interest. For both amplitude modulation and frequency modulation, the film clearly demonstrates the ability of the system to differentiate betweeen modulation by voice and modulation by music. Oral pauses are clearly indicated by the absence of modulation and the resultant straight line trace of the display.

An excellent example of multi-tone FSK is included as well as the more common two-level signal. In both cases, extremely rapid frequency-selective fading is evidenced by rapid changes in amplitude of the individual straight line traces corresponding to the discrete frequencies contained in the signal format.

The rippled, watery-like appearance of a single-sideband signal is demonstrated. Included also is a sequence showing a multi-tone double-sideband suppressed-carrier signal indicating first modulation by a single sinusoid, then a rapid burst of frequency shifts of the modulating signal, and then the modulating signal reverting to a single sinusoid. Individual parallelograms, each corresponding to modulation by a sinusoid of a different frequency, are evident.

In all the sequences photographed, a distinctive display is produced which corresponds to the form determined analytically. This film strip is available upon request from Prof. G. A. Myers, Naval Postgraduate school, Monterey, California.

IV. CONCLUSIONS AND RECOMMENDATIONS

A. CONCLUSIONS

Conclusions concerning the capabilities and possible uses of the linear polar-display signal analyzer are as follows:

(1) The LPD system produces a distinctive display for each of the following types of radio signals:

a. simultaneous sinusoids
b. full-carrier amplitude modulation
c. on-off keying (continuous-wave)
d. pulse amplitude modulation
e. double-sideband suppressed-carrier
f. single-sideband AM
g. angle modulation by an analog signal
h. frequency-shift keying
i. phase-shift keying.

(2) In addition to the information concerning type of modulation, the LPD system provides a measure of various signal parameters such as average carrier frequency, carrier envelope, bandwidth, duty factor (pulsed signals), instantaneous frequency, and the amount of phase shift for phase-shift-keyed signals.

(3) The LPD system also provides a means for measuring the normalized autocorrelation function of a bandpass gaussian process.

(4) The LPD system may be useful in signal monitoring applications. For example, it provides a simple and convenient indication of incidental AM on the output of an FM transmitter or of incidental FM on the output of an AM transmitter.

(5) The LPD system may be useful in systems where operator recognition and identification of signals is desirable.

B. RECOMMENDATIONS

Several additional areas of investigation and possible methods of improving the capability of the present system are listed here.

(1) Use an oscilloscope having a variable or extendable retentivity, (memoscope) to increase the recognition capability for digital communication signals having a low data rate or radar signals having a low duty cycle.

(2) Investigate the feasibility of using the LPD system in conjunction with a scanning receiver and an automatic camera, triggered by a level detector, to conduct an automatic cataloging operation in a high density signal environment.

(3) Attempt to improve the recognition capability of the system in the case of single-sideband signals.

APPENDIX A

CIRCUIT DIAGRAMS

This appendix presents the detailed circuit diagrams for the amplifier and impedance-matching circuits used in the linear polar display system and the modulators used to generate some of the signals used to evaluate the LPD system operation.

The system and modulators are presented in block diagram form in Fig. A-1. As indicated, inputs to the system can be obtained from the several modulators shown for the investigation of known signals, or from an R-390 receiver for the study of live signals in the HF band.

A. MODULATORS

1. Frequency Modulator

The frequency modulator circuit is shown in Fig. A-2. This circuit is also used to provide the 455 kHz carrier for the amplitude modulator, the phase shift modulator, and the double-sideband suppressed-carrier modulator. The circuit of Fig. A-2a is basically an astable multivibrator, but the resistors through which current normally flows to charge capacitors C_1 and C_2 have been replaced by PNP transistors in series with moderately large resistors (R_1 = 10K) to provide a regulated, constant charging current.

The relationship of the frequency of oscillation to the magnitude of the charging current can be explained with the aid of Fig. A-2b which shows the voltage waveform at the base of T_1. The waveform of Fig. A-2b is produced by the constant current source charging C_1 during that part of a cycle when T_1 is cut off. The waveform differs from the standard

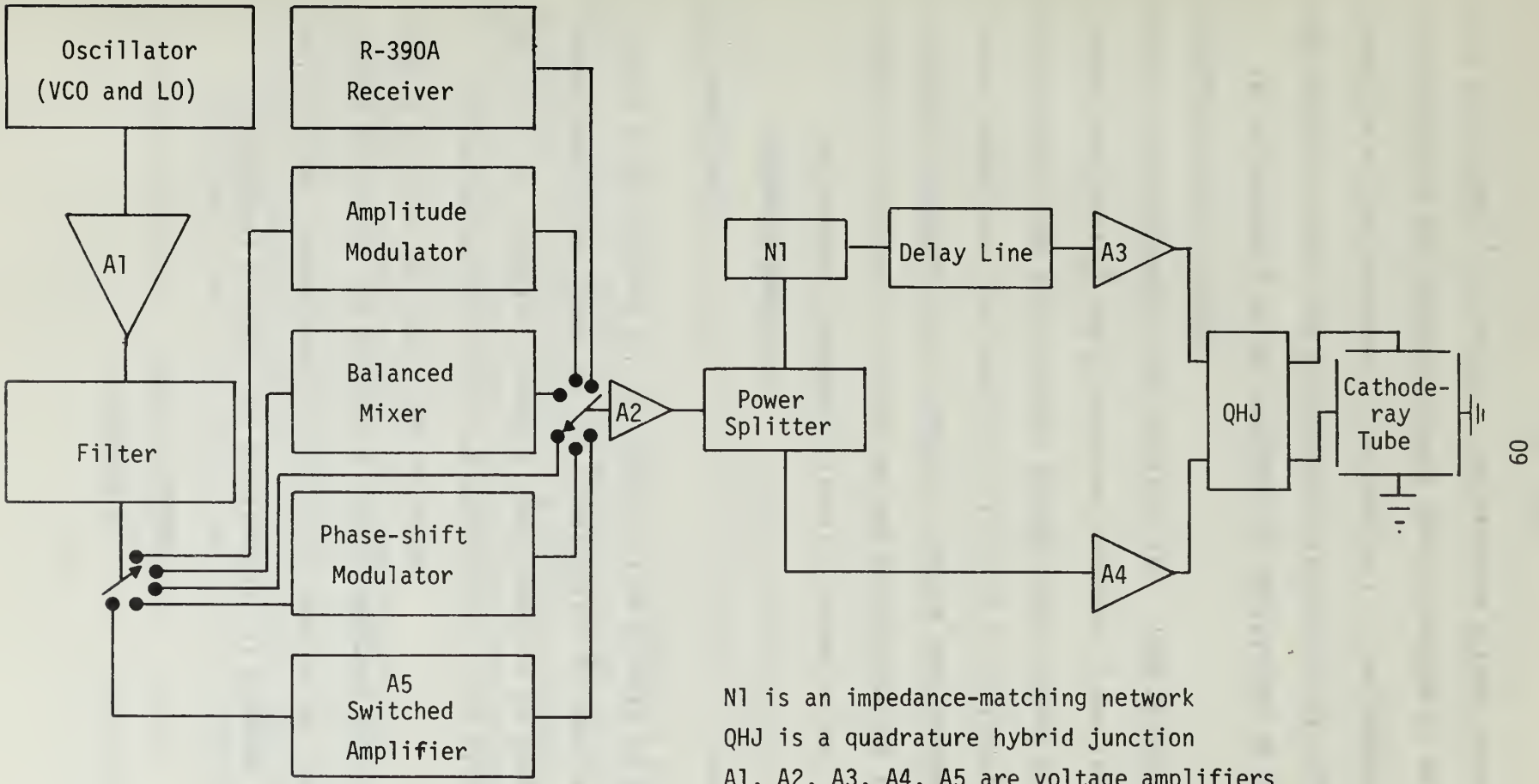

FIG. A-1. BLOCK DIAGRAM OF THE LPD SYSTEM AND SIGNAL SOURCES.

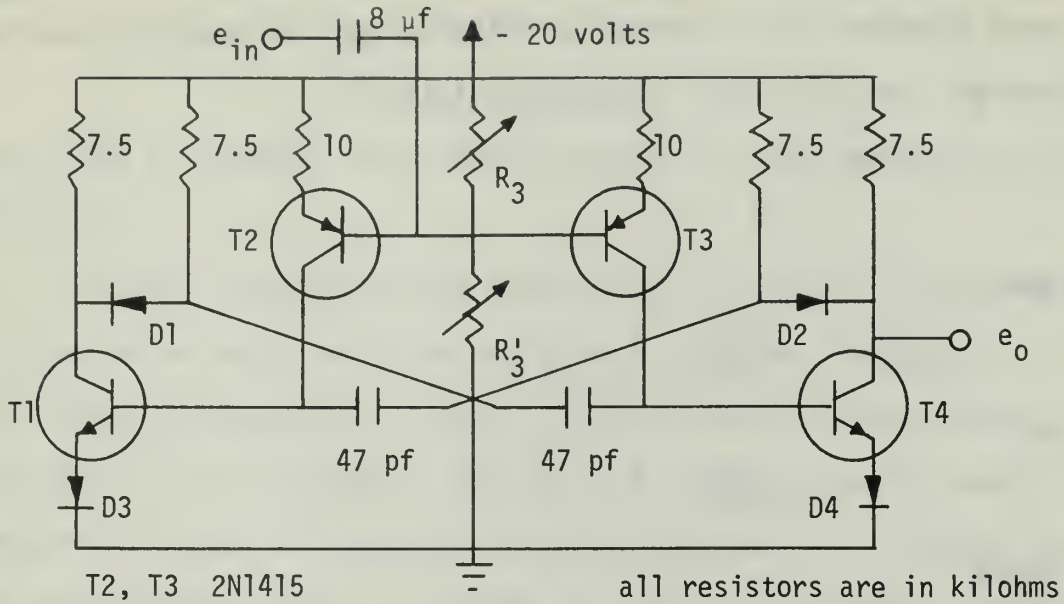

T2, T3 2N1415
T1, T4 2N4420
$R_3 + R_3' = 7$ kΩ

all resistors are in kilohms
all diodes are 1N276

a. Circuit diagram.

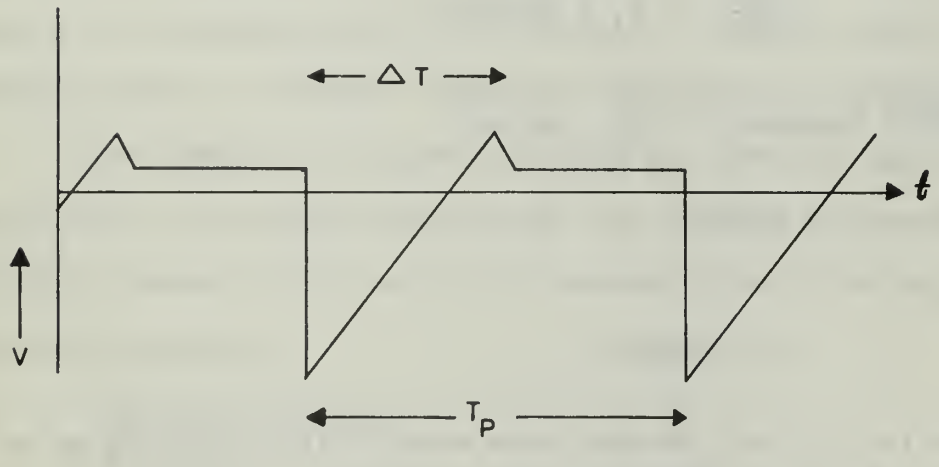

b. Voltage waveform at the base of transistor T1.

FIG. A-2. FREQUENCY MODULATOR.

base waveform for an astable multivibrator only in that the capacitor charges linearly rather than exponentially.

Since

$$CV = q \tag{A-1}$$

and

$$C \frac{dV}{dt} = I \tag{A-2}$$

or

$$C \frac{\Delta V}{\Delta T} = I \tag{A-3}$$

where

$$\Delta T = \frac{T_p}{2} \tag{A-4}$$

and T_p is the period of oscillation, then

$$\frac{2C\Delta V}{T_p} = I, \text{ a constant.} \tag{A-5}$$

In terms of frequency $f = \frac{1}{T_p}$, we have

$$2C\Delta Vf = I \tag{A-6}$$

or

$$f = \frac{I}{2C\Delta V} . \tag{A-7}$$

As shown in Fig. A-2a the modulating signal $e_i(t)$ is applied at the bases of T_2 and T_3. Therefore,

$$I = \frac{h_{fe} e_i R_b}{z_{23} + R_b} = Ke_i \tag{A-8}$$

where z_{23} is the impedance seen looking into the base of T_2 or T_3, h_{fe} is the forward current transfer ratio of the transistor with the emitter grounded, R_b is the equivalent resistance of R_3 and R_3' in parallel and K is a constant. Substituting Eq. (A-8) into Eq. (A-7)

gives

$$f = \frac{Ke_i}{2C\Delta V} . \qquad \text{(A-9)}$$

Hence, the frequency of oscillation is linearly related to the modulating voltage e_i.

Diodes D_1 and D_2 prevent the capacitors C_1 and C_2 from charging through the collector resistors and serve to make the frequency of oscillation independent of the load. Diodes D_3 and D_4 prevent zener breakdown of the base-emitter junction of T_1 and T_2 since the reverse breakdown voltage for the emitter base junction with the collector open for the transistors used is -5 volts and the base voltage of T_1 and T_2 can approach -15 volts without D_3 and D_4.

The static frequency-versus-voltage characteristic of the circuit of Fig. A-2 is shown in Fig. A-3. The characteristic is slightly concave upwards over the range 100 kHz to 1 Mhz, but is nearly linear over the frequency range of interest. Modulator sensitivity is 195 $\frac{kHz}{volt}$.

The lowpass filter used to convert the collector wave form generated by the astable multivibrator to a constant amplitude sinusoidal voltage is shown in Fig. A-4. It is composed of two m-derived L sections and one pi section.

2. Amplitude Modulator

The amplitude modulator circuit is shown in Fig. A-5. The circuit is a tuned, common-emitter amplifier. The modulating signal is applied to the emitter, thereby modulating the operating point of the amplifier and hence its voltage gain. The carrier is applied at the base of the transistor. Capacitor C_2 provides a low impedance path to the 455 kHz carrier voltage and a high impendance to the modulating signal. Resistor R_1 limits the input signal level to prevent saturation of the amplifier.

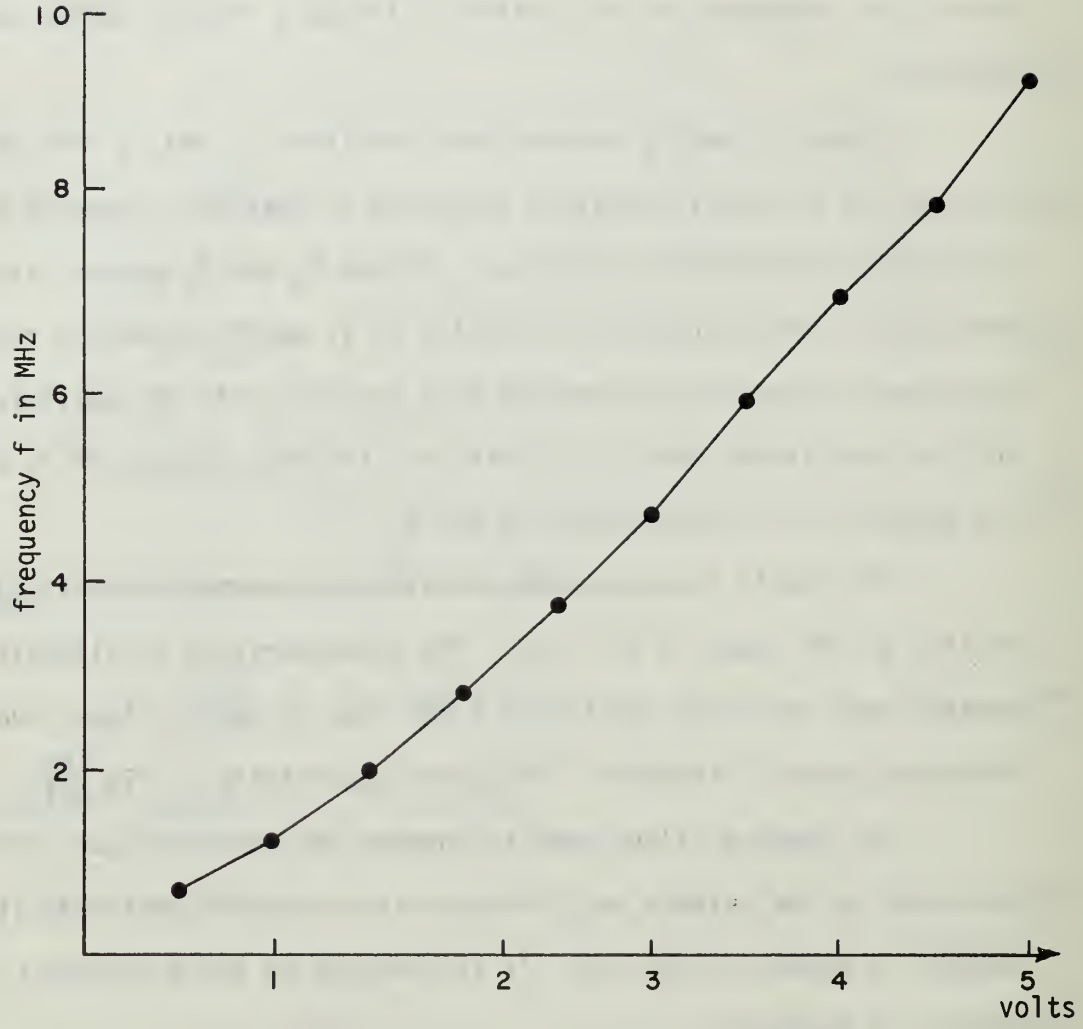

FIG. A-3. STATIC FREQUENCY-VS-VOLTAGE CHARACTERISTIC OF THE FREQUENCY MODULATOR.

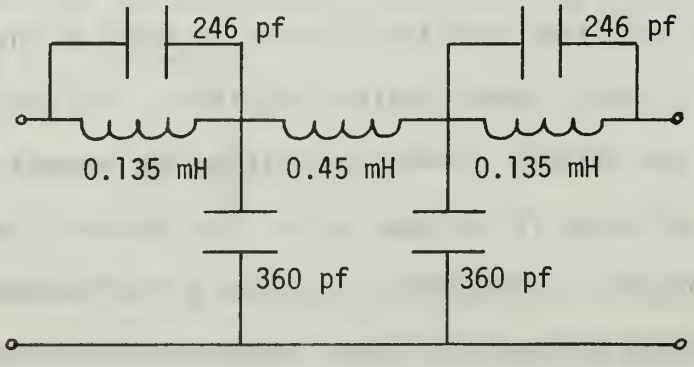

FIG. A-4. LOWPASS FILTER CIRCUIT DIAGRAM.

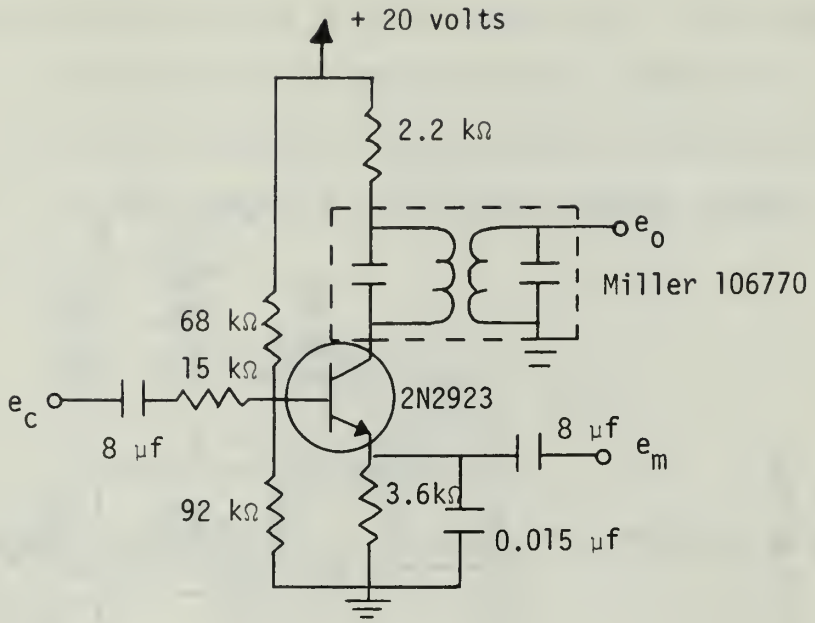

FIG. A-5. AMPLITUDE MODULATOR CIRCUIT DIAGRAM.

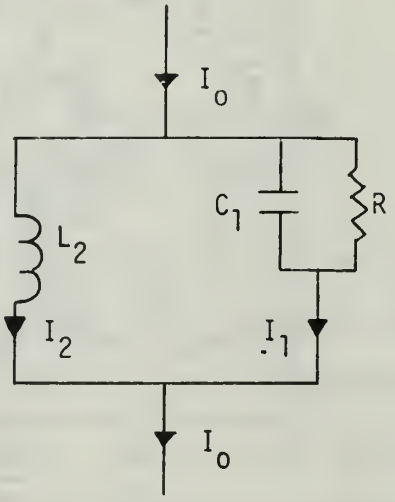

FIG. A-6. PHASE MODULATOR EQUIVALENT CIRCUIT.

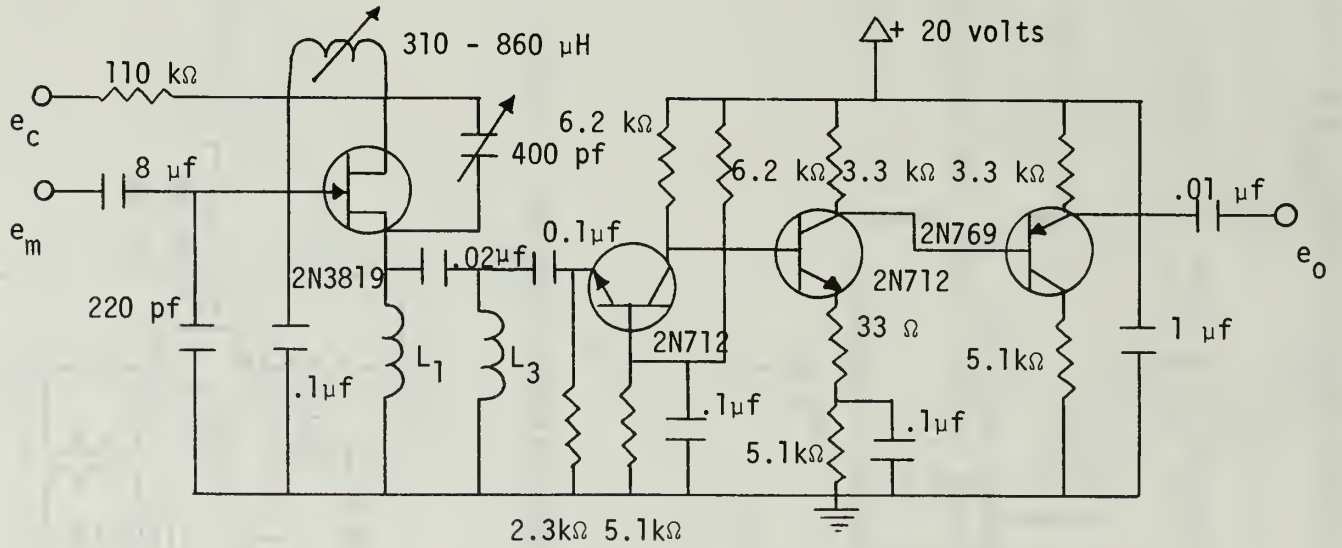

FIG. A-7. PHASE MODULATOR CIRCUIT DIAGRAM.

3. Phase Modulator

The phase modulator used is a modification of a circuit developed by the Apollo Support Department of General Electric Company [Ref. 12]. The modulator operating principle can be explained by considering the circuit of Fig. A-6. The following relationship between currents I_1 and I_0 in Fig. A-7 can be derived:

$$\frac{I_1}{I_0} = \frac{1 + \omega^2 C_1{}^2 R^2}{1 + (\omega C_1 - \frac{1}{\omega L_2})^2 R^2} \quad e^{j\phi} \tag{A-10}$$

where ω is radian frequency and ϕ is the phase of I_0 relative to that of I_1. Further, if

$$L_2 = \frac{1}{2\omega^2 C_1} \tag{A-11}$$

then Eq. (A-10) becomes

$$\frac{I_1}{I_0} = e^{j\phi} \tag{A-12}$$

where

$$\phi = 2 \arctan \omega C_1 R. \tag{A-13}$$

The phase ϕ can be varied by varying C_1 or R or both.

A field effect transistor (FET) is used as the variable resistance element in the circuit of Fig. A-6. The original circuit used a P-channel FET, the RCA TA 2330. Since a linear phase-versus-gate-voltage characteristic is required, the transistor is biased to utilize the tangent-like relation of dynamic output resistance to gate voltage to compensate for the arctangent relation expressed in Eq. (A-13). In the present application, a phase-shift-keyed signal is desired and so continuous linearity is not required.

An N channel FET, the 2N3819 is utilized in the final circuit configuration. No dc bias is applied to the FET; that is, $V_{gs} = 0$ where V_{gs} is the gate-to-source voltage. Modulation is achieved by applying negative pulses to the FET gate, thereby increasing the channel resistance of the transistor.

In Fig. A-7, C_1, L_2, and T_1 form the basic modulator circuit represented by Fig. A-6. Capacitor C_4 places one end of L_2 at RF ground yet isolates the drain of T_1 from dc ground. The components L_1, C_5, and L_3 couple the phase-modulated current to the common base amplifier T_2 which has a low input impedance. Inductor L_1 also maintains the dc voltage of the source of T_1 at ground level. Stages T_3 and T_4 provide additional gain and, as originally designed, provided an impedance match to a phase detector. These three amplifier stages are compatible with the rest of the system and perform well at 455 kHz; they were incorporated into the system in their original form. The circuit is able to provide phase shifts continuously from zero degrees to about 170 degrees.

4. Balanced Mixer

Generation of all suppressed-carrier signals was done using the Relcom M1C balanced mixer whose circuit diagram is shown in Fig. A-8.

B. AMPLIFIERS AND IMPEDANCE-MATCHING CIRCUITS

Several types of amplifiers are used throughout the system. These amplifiers are used primarily to provide isolation and for impedance matching. For example, the power splitter and the quadrature hybrid junction are 50 ohm devices, and the delay line requires 100 ohms at both input and output; the delayed signal requires two impedance-level changes.

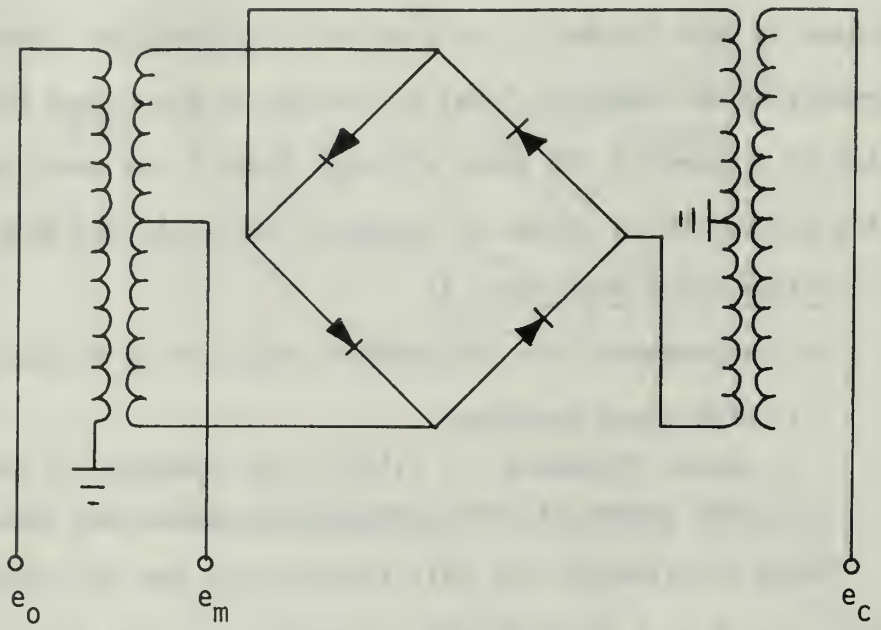

FIG. A-8. BALANCED MIXER CIRCUIT DIAGRAM.

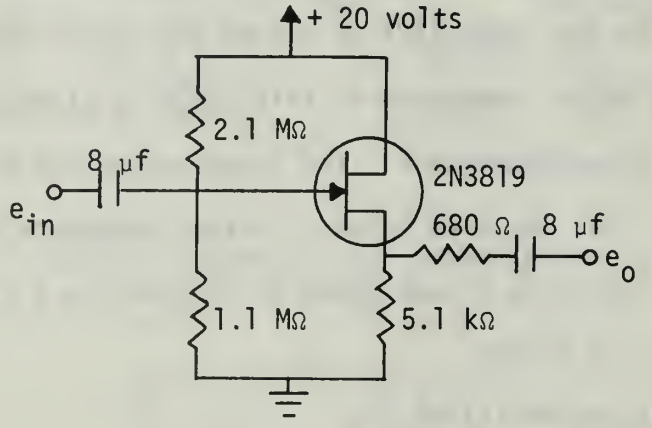

FIG. A-9. CIRCUIT DIAGRAM OF THE FILTER INPUT AMPLIFIER A1.

Because of the additional requirement that there be no frequency-dependent phase differences between the two channels, identical amplifiers are placed in each channel. For example, the undelayed signal is converted from an impedance level of 50 ohms at the output of the power splitter to a level of 100 ohms, although there is no need for this other than the corresponding change of impedance levels in the delayed channel.

1. Filter Input Amplifier, A1

The requirements for this buffer stage are as follows:

1. high input impedance
2. output impedance = 1 kilohm, the impedance of the filter
3. high degree of isolation between output and input.

These requirements are well satisfied by the FET common-drain stage shown in Fig. A-9. In this application, the fact that the output impedance of this amplifier is relatively independent of the impedance of the signal source is particularly attractive since the source is the astable multivibrator and hence has an output impedance level which is determined by the state (off or on) of the output transistor.

The output impedance of this stage is given by $\frac{1}{g_{fs}}$ where g_{fs} is the FET transconductance. The transconductance for the device is 3400 μmhos. The measured value of output impedance was found to be 300 ohms. Therefore R_4 was added to achieve the 1 kilohm impedance level required by the filter.

2. Switched Amplifier, A5

The amplifier shown in Fig. A-10 is used in the analysis of pulsed signals. The device consists of the common-source amplifier T_2 which provides a gain of 2. The input to T_2 is switched by T_1. The resistor R_2 forward biases the base emitter junction of T_1 so that the input signal is attenuated by the voltage divider consisting of R_1 and

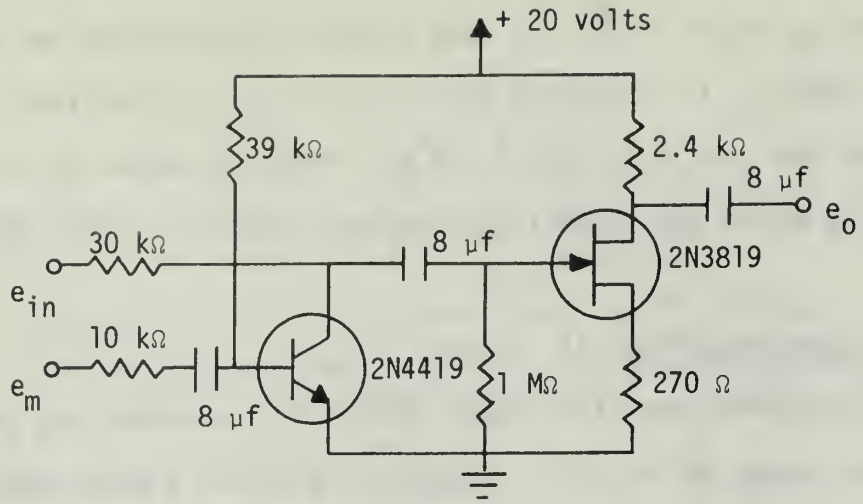

FIG. A-10. CIRCUIT DIAGRAM OF THE SWITCHED AMPLIFIER A5.

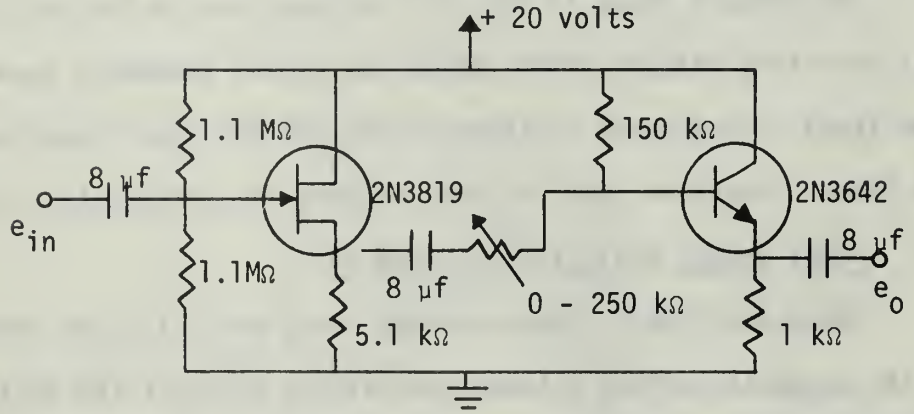

FIG. A-11. CIRCUIT DIAGRAM OF THE OUTPUT AMPLIFIER A2.

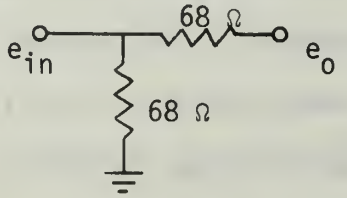

FIG. A-12. CIRCUIT DIAGRAM OF THE IMPEDANCE-MATCHING NETWORK N1.

r_{ce} where r_{ce} is the resistance seen between the collector and emitter of T_1. Since r_{ce} is negligible with respect to R_1, effectively no signal arrives at the gate of T_2 when T_1 is on. Negative pulses at the base of T_1 turn the switch off, permitting the input signal to reach the gate of T_2.

3. Output Amplifier, A2

This buffer amplifier shown in Fig. A-11 precedes the power splitter as shown in Fig. A-1. The device provides a high input impedance of approximately 300 kilohm, variable attenuation by means of the potentiometer R_7, and a low output impedance of approximately 30 ohms.

4. Impedance Matching Network, N1

The network shown in Fig. A-1 and detailed in Fig. A-12 is a purely resistive network which raises the signal impedance level from the 50 ohm level of the power splitter to the 100 ohm level required by the delay line. Insertion loss for this network is approximately 7 dB.

5. Final Output Amplifiers, A3 and A4

These amplifiers, shown in Figs. A-13 and A-14, are identical with the exception of the attenuation network R_1-R_2 of the amplifier in the undelayed channel. The insertion loss due to the delay line varies from a negligible amount at 0 μs delay to about 5 dB at a setting of 90 μs. The variable resistor, R_2, is adjusted manually to equalize the signal level in both channels. This network is similar to network N1.

Stage T_1 is a common-source FET amplifier providing an input impedance of 100 ohms and a voltage gain of 4. Stage T_2 is a common-collector amplifier providing exactly the 50 ohm output required for impendance matching to the quadrature hybrid junction.

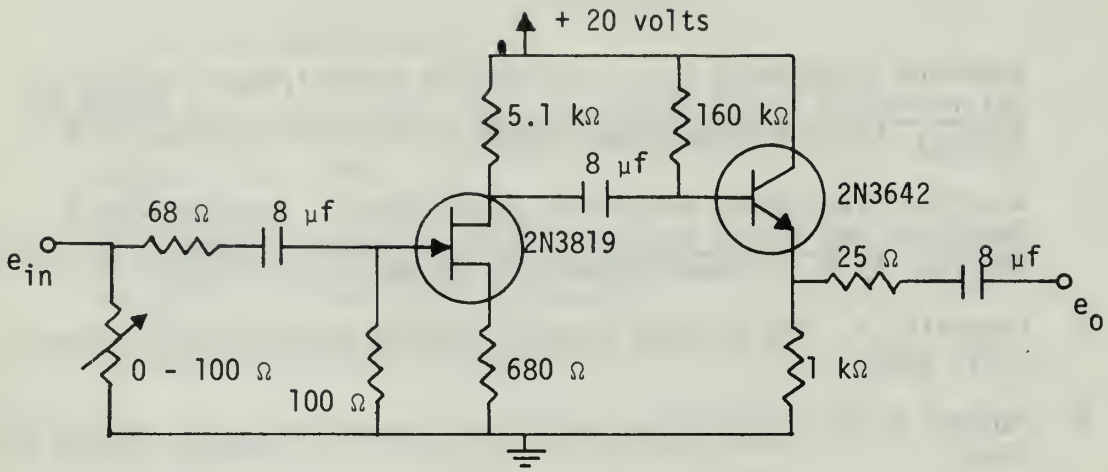

FIG. A-13. CIRCUIT DIAGRAM OF THE FINAL OUTPUT AMPLIFIER A3.

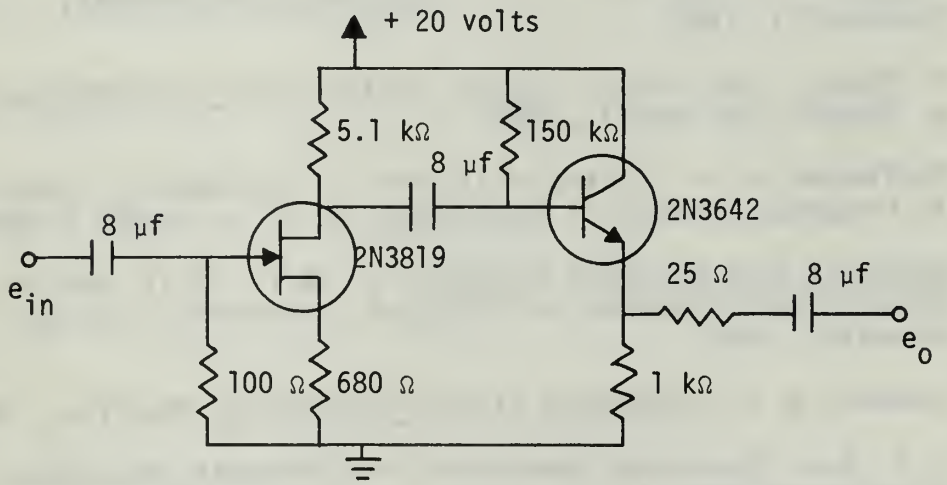

FIG. A-14. CIRCUIT DIAGRAM OF THE FINAL OUTPUT AMPLIFIER A4.

REFERENCES

1. Stanford Electronics Laboratory Report 1905-2/1709-3, Theory of Polar-Display Signal Analyzers, and a Radio Direction-Finding Analogy, by G. A. Myers, March 1968.

2. Stanford Electronics Laboratory Report 1905-1, Performance of Receivers and Signal Analyzers Using Broadband Frequency Sensitive Devices, by R. C. Cumming and G. A. Myers, March, 1967.

3. Papoulis, A., The Fourier Integral and Its Applications, McGraw-Hill, 1962.

4. Panter, P. F., Modulation, Noise and Spectral Analysis, McGraw-Hill, 1965.

5. Schwartz, M., Information Transmission, Modulation and Noise, McGraw-Hill, 1959.

6. Fundamentals of Single-Sideband, 2nd ed., p. 1-1 - 1-17, Collins Radio Company, 1959.

7. Terman, F. E. and Petit, J. M., Electronic Measurements, p. 230-288, McGraw-Hill, 1952.

8. Millman, J. and Taub, H., Pulse, Digital, and Switching Waveforms, p. 404-451, McGraw-Hill, 1965.

9. Biddlecomb, R. W., "Latest Multivibrator Improvement, Linear Voltage to Frequency Converter," Electronics, v. 36, p. 64-65, 26 April, 1963.

10. Reference Data For Radio Engineers, p. 10-1 - 10-11, 5th ed., International Telephone and Telegraph Corporation, Judd and Detweiler, 1968.

11. Cochrun, B. L., Transistor Circuit Engineering, Macmillan, 1967.

12. U. S. Army Electronics Laboratory, Fort Monmouth, New Jersey, Interference Reduction Techniques for Nonlinear Devices, by J. C. Otto and R. R. Garcia, 15 May, 1964.

INITIAL DISTRIBUTION LIST

		No. Copies
1.	Library, Code 0212 Naval Postgraduate School Monterey, California 93940	2
2.	Commandant of the Marine Corps (Code A03C) Headquarters, USMC Washington, D. C. 20380	1
3.	Assoc. Professor Glen A. Myers, Code 52Mv Department of Electrical Engineering Naval Postgraduate School Monterey, California 93940	1
4.	Major N. J. Spitzer 1145 Division St. Green Bay, Wisconsin 54303	1
5.	James Carson Breckinridge Library Marine Corps Development and Educational Command Quantico, Virginia 22134	1

DOCUMENT CONTROL DATA - R & D

(Security classification of title, body of abstract and indexing annotation must be entered when the overall report is classified)

1 ORIGINATING ACTIVITY *(Corporate author)*

Naval Postgraduate School
Monterey, California 93940

2a. REPORT SECURITY CLASSIFICATION

Unclassified

2b. GROUP

3 REPORT TITLE

Experimental Evaluation of a Linear Polar-Display Signal Analyzer

4. DESCRIPTIVE NOTES *(Type of report and inclusive dates)*

Electrical Engineer's Thesis - June 1969

5. AUTHOR(S) *(First name, middle initial, last name)*

Norbert J. Spitzer Major U.S. Marine Corps

6. REPORT DATE	7a. TOTAL NO. OF PAGES	7b. NO. OF REFS
June 1969	76	12

8a. CONTRACT OR GRANT NO.	9a. ORIGINATOR'S REPORT NUMBER(S)
b. PROJECT NO.	
c.	9b. OTHER REPORT NO(S) *(Any other numbers that may be assigned this report)* None
d.	

10. DISTRIBUTION STATEMENT

Distribution of this document is unlimited.

11. SUPPLEMENTARY NOTES	12. SPONSORING MILITARY ACTIVITY
	Naval Postgraduate School Monterey, California 93940

13. ABSTRACT

This report presents the results of an experimental evaluation of a linear, polar-display signal analyzer. Signals generated in the laboratory are used to determine the ability of the device to indicate the type of carrier modulation and the carrier parameters such as frequency, data rate, and bandwidth. Live signals in the HF band are monitored by applying the predetected output of an R-390A receiver directly to the signal analyzer.

Photographs of the actual displays resulting from signals generated in the laboratory demonstrate the ability of the system to provide a distinctive display in each case. Various parameters of the input signal can be determined by measuring parameters of the display. A twelve-minute movie indicates the system performance in the case of live signals. The ability of the signal analyzer to determine the normalized autocorrelation function of a bandpass gaussian process is demonstrated.

14 KEY WORDS	LINK A		LINK B		LINK C	
	ROLE	WT	ROLE	WT	ROLE	WT
Frequency Measurement						
Parallel-Channel Systems						
Polar-Display Systems						
Signal Analyzers						
Spectrum Monitors						